CELL BIOLOGY

The 40S-LARP1 complex reprograms the cellular translatome upon mTOR inhibition to preserve the protein synthetic capacity

Pedro Fuentes[1]†, Joffrey Pelletier[1]†‡, Carolina Martinez-Herráez[1,2], Virginia Diez-Obrero[3,4,5,6], Flavia Iannizzotto[1], Teresa Rubio[1], Marta Garcia-Cajide[1], Sandra Menoyo[1], Victor Moreno[1,3,4,5,6,7], Ramón Salazar[1,4,5], Albert Tauler[1,2], Antonio Gentilella[1,2]*

Ribosomes execute the transcriptional program in every cell. Critical to sustain nearly all cellular activities, ribosome biogenesis requires the translation of ~200 factors of which 80 are ribosomal proteins (RPs). As ribosome synthesis depends on RP mRNA translation, a priority within the translatome architecture should exist to ensure the preservation of ribosome biogenesis capacity, particularly under adverse growth conditions. Here, we show that under critical metabolic constraints characterized by mTOR inhibition, LARP1 complexed with the 40S subunit protects from ribophagy the mRNAs regulon for ribosome biogenesis and protein synthesis, acutely preparing the translatome to promptly resume ribosomes production after growth conditions return permissive. Characterizing the LARP1-protected translatome revealed a set of 5′TOP transcript isoforms other than RPs involved in energy production and in mitochondrial function, among other processes, indicating that the mTOR-LARP1-5′TOP axis acts at the translational level as a primary guardian of the cellular anabolic capacity.

INTRODUCTION

The production of cellular mass is a prerequisite for cell replication as it endows the daughter cells with molecular machineries essential to execute the inherited genetic information. Ribosomes play a key role in this process based on their ability to synthesize new proteins, and an increase in their numbers is critical to undergo cell replication (*1*). To maintain cellular homeostasis, the rate of protein synthesis is dynamically controlled by specific factors that sense external and internal cues, including nutrient availability, oxygen accessibility, and energetic status, all acting to determine the equilibrium between anabolic and catabolic cellular processes (*2*). To a large extent, the tight communication among sensors and effectors is mediated by the mammalian target of rapamycin (mTOR) kinase, which acts to coordinate the overall metabolic balance in the cell (*3*). This circuitry is central for the cell to adapt to acute changes in extracellular or intracellular conditions or to differentiate the metabolic needs of specific cell types in distinct tissues and organs (*4*).

Upon nutritional limitations, mTOR acts as a metabolic switch to lower global metabolism. Many inhibitory growth stimuli are characterized by an overall reduction of mTOR signaling, and, more recently, it was observed that prolonged mTOR inhibition triggers the selective degradation of cellular ribosomes, in a process termed ribophagy (*5*). A reduction in the number of available ribosomes, along with the protein synthetic capacity, alters the repertoire of cellular transcripts engaged in translation, modifying the translational program of the cell. To reestablish the anabolic demand required to awaken from a low metabolic state, cells must preserve the ability to quickly generate new ribosomes and reconstitute the protein synthetic capacity, a process that, in higher metazoans, is largely controlled at the translational level (*6*, *7*). This poses the question of whether the transcriptome has an innate translational hierarchy that serves to prioritize basic cellular biosynthetic routes under critical metabolic constraints.

The intrinsic plasticity of the translatome has been observed in a number of biological circumstances to rapidly respond to cellular perturbations. To this end, higher eukaryotes have evolved an arsenal of mechanisms to selectively translate stress mRNAs in response to sudden changes (*8*–*14*). However, under chronic metabolic limitations, little is known of whether the transcriptome has a hierarchically defined translational design, which could arise to preserve the anabolic capacity of the cell. In support of this hypothesis, it was previously observed that $CD34^+$ hematopoietic progenitors, where global mTOR signaling and the protein synthesis rate are strongly restrained (*4*, *15*), have the ability during the process of erythropoiesis to convert the anabolic potential stored in the form of mRNA into functional ribosomes (*15*–*17*). Similar to HSCs, other stem cell compartments showed a similar protein synthesis fingerprint in quiescence and during differentiation (*18*, *19*). Likewise, the dependency of the zygote on the maternal translational apparatus during the first stages of development rapidly declines when the cellular reservoir of ribosomal protein (RP) mRNAs is engaged in translation to produce new ribosomes (*20*).

Recently, the RNA binding protein LARP1 (La-related protein 1), a germline determinant in *Caenorhabditis elegans* (*21*), has been placed at the crossroad of mTOR signaling and the process of ribosome biogenesis based on the evidences that the 5′TOP element of RP mRNAs

[1]Laboratory of Cancer Metabolism, ONCOBELL Program, Bellvitge Biomedical Research Institute (IDIBELL), Barcelona, Spain. [2]Department of Biochemistry and Physiology, Faculty of Pharmacy and Food Science, University of Barcelona, Barcelona, Spain. [3]Unit of Biomarkers and Susceptibility, Oncology Data Analytics Program, Catalan Institute of Oncology (ICO). Hospitalet de Llobregat, Barcelona, Spain. [4]Consortium for Biomedical Research in Epidemiology and Public Health (CIBERESP), Spain. [5]Department of Clinical Sciences, Faculty of Medicine, University of Barcelona, Barcelona, Spain. [6]Colorectal Cancer Group, ONCOBELL Program, Bellvitge Biomedical Research Institute (IDIBELL). L'Hospitalet de Llobregat, Barcelona, Spain. [7]Consortium for Biomedical Research in Oncology (CIBERONC), Spain.
*Corresponding author. Email: agentilella@idibell.cat, antonio.gentilella@ub.edu
†These authors contributed equally to this work.
‡Present address: Institute for Research in Biomedicine (IRB Barcelona), Barcelona Institute of Science and Technology (BIST), Baldiri i Reixac 10, 08028 Barcelona, Spain.

is selectively bound by LARP1 complexed with the 40*S* ribosomes to stabilize this family of transcripts (*22*). Despite the controversies of whether LARP1 is a translational repressor or an activator of 5′TOP mRNAs (*23*, *24*), it is quite well established that LARP1 is a phospho-target of mTOR, and some of its most recurrent phoshpo-acceptor residues have been identified by multiple studies (*25*–*28*).

Here, we show that chronic mTOR inhibition, either by pharmacological treatment or by nutrient deprivation, reprograms the cell's translatome to preserve its potential of rapidly reconstituting the anabolic capacity when appropriate conditions are reestablished. Mechanistically, despite the decline of total ribosome content upon prolonged inhibition of mTOR, the 40*S* ribosomes complexed with the RNA binding protein LARP1 selectively mediate the preservation in a translationally inactive state of 5′TOP mRNAs family. Such reservoir can be rapidly used by the protein synthetic machinery when mTOR signaling is reactivated, acutely increasing the production of new ribosomes and the protein synthetic rate, thus resetting the proliferative capacity of the cell. RNA sequencing (RNA-seq) coupled with transcriptional start site (TSS) analyses of the pool of transcripts controlled by mTOR-LARP1 axis revealed the presence of the vast majority of ribosome biogenesis and protein synthesis constituents as well as a new subset of 5′TOP mRNAs belonging to metabolic pathways necessary to up-regulate cellular anabolism. These observations led us to the finding that the translational network defined by the *cis* 5′TOP motif and by mTOR status constitutes an mRNA regulon that serves to rapidly preserve and to reactivate the anabolic capacity of the cell, with LARP1 acting as the guardian of the ribosome biogenesis and protein synthesis at the translational level.

RESULTS

Chronic mTOR inhibition increases 5′TOP mRNA stability and reduces non-TOP mRNA levels

We recently demonstrated that a specific subset of 40*S* native ribosomes complexed with the RNA binding protein LARP1 has a selective affinity for RP mRNAs and the broader 5′TOP family of transcripts and that acute treatment with the mTORC1 allosteric inhibitor rapamycin drives the formation of the complex (*22*). As chronic exposure to mTOR inhibitor accelerates the turnover of cellular ribosomes (*5*), we reasoned that the representation of 5′TOP mRNAs associated with the translational machinery would increase over time of mTOR inhibition by virtue of the 40*S*-LARP1 complex. To verify this hypothesis, we treated HCT116 colorectal cells with the mTOR adenosine 5′-triphosphate (ATP) site competitive inhibitor TAK228 at 250 nM (fig. S1A), a concentration that increased the cells in G_0-G_1 cell cycle phase (fig. S1B), and monitored over time the expression of a number of 5′TOP and non-TOP mRNAs. As shown in Fig. 1A, total levels of RPs RPS6, RPL5, and RPL11 mRNAs were maintained or slightly increased at 24 and 48 hours of treatment when normalized to cell number, whereas non-TOP mRNAs, such as β-actin, displayed the opposite trend, a progressive reduction of their levels over time. CRISPR-Cas9 knockout (KO) of LARP1 in HCT116 cells abrogated the preservation of RP mRNAs upon chronic exposure to TAK228 and phenocopied the reduction observed for the non-TOP mRNAs (Fig. 1A and fig. S1A). Consistent with enhanced ribosome turnover by prolonged mTOR inhibition (*5*) (fig. S1C), we found that the ratio between 5′TOP mRNAs and available ribosomes augmented over time of treatment as opposed to non-TOP mRNAs (fig. S1D), suggesting that chronic inhibition of mTOR modifies the repertoire of available transcripts per cellular ribosome content in favor of 5′TOP mRNAs and that LARP1 is critical in executing this selective protection. This observation was not limited to colorectal cancer cells HCT116 as A549 lung adenocarcinoma cells also recapitulated the LARP1-dependent 5′TOP protection and the destabilization of non-TOP mRNAs (fig. S1E). Of note, reducing the concentration of TAK228 to 50 nM in RT4 bladder carcinoma cells, which were reported to be exquisitely sensitive to TAK228 (*29*), and in HCT116 cells was sufficient to preserve 5′TOP mRNAs and to reduce non-TOP mRNAs upon mTOR inhibition (fig. S1F), suggesting that cells are particularly responsive to this mechanism. Moreover, the effects produced by prolonged pharmacological mTOR inhibition appeared to be specific to mTOR signaling as mTORC1 allosteric inhibitor rapamycin also recapitulated the effects of the ATP-site inhibitor TAK228 (fig. S1G).

As many negative growth stimuli operating in physiological contexts inhibit mTOR signaling (*3*), we sought to investigate how chronic exposure to these conditions affected the representation of 5′TOP and non-TOP mRNAs in the cell. Strikingly, serum deprivation, a well-characterized mTOR-inhibiting paradigm (fig. S1H), recapitulated over time the observations obtained with direct mTOR inhibition (Fig. 1B and fig. S1J). Likewise, chronic exposure to other mTOR-inhibiting stimuli such as amino acid deprivation (fig. S1K) or oxygen limitation (fig. S1L) increased the ratio of 5′TOP mRNA/18*S* ribosomal RNA (rRNA) only in LARP1-expressing cells (Fig. 1C). Again, β-actin mRNA was found reduced irrespective of LARP1 expression upon all mTOR-inhibiting stimuli tested.

The hypothesis that the LARP1 expression preserves the levels of 5′TOP mRNAs in the cell upon mTOR inhibition suggests that, in these conditions, the 5′TOP motif confers an increased mRNA stability. By means of an HCT116 Tet-inducible 5′TOP reporter cell line, which we recently described (*22*), we found that when cells were exposed chronically to the mTOR inhibitor TAK228 or to amino acid deprivation, the stability of 5′TOP–β-globin reporter mRNA was markedly enhanced when compared to cells maintained under normal growing conditions, whereas a significant decrease in stability of the mutant 5′TOP reporter mRNA was observed following the same treatments (Fig. 1D). These results are consistent with the total RNA levels of endogenous 5′TOP and non-TOP mRNAs observed under the same conditions (Fig. 1, A and C), suggesting that the 40*S*-LARP1 stability complex mediates 5′TOP accumulation. In support of this hypothesis, knockdown of RPS6, which impairs the synthesis of native 40*S* ribosomes (*22*, *30*), hampered the preservation of 5′TOP mRNAs triggered by TAK228, with no effect on β-actin and AMD1 (adenosylmethionine decarboxylase 1) non-TOP mRNA levels, confirming that the 40*S* subunit and LARP1 are both required for 5′TOP mRNA stability induced by prolonged mTOR inhibition (Fig. 1E and fig. S1M). Conversely, reducing the synthesis of 60*S* ribosomes, which results into a higher availability of free 40*S* ribosomes and drives the formation of 40*S*-LARP1-5′TOP complex (*22*), saturated the ability of chronic TAK228 treatment to induce further accumulation of 5′TOP mRNAs at the total level (fig. S1N). Together, these results indicate that chronic mTOR inhibition, either by pharmacological treatment or by nutrient deprivation, reshape the transcriptome representation by increasing the 5′TOP mRNAs stability and by decreasing the stability of non-TOP mRNAs.

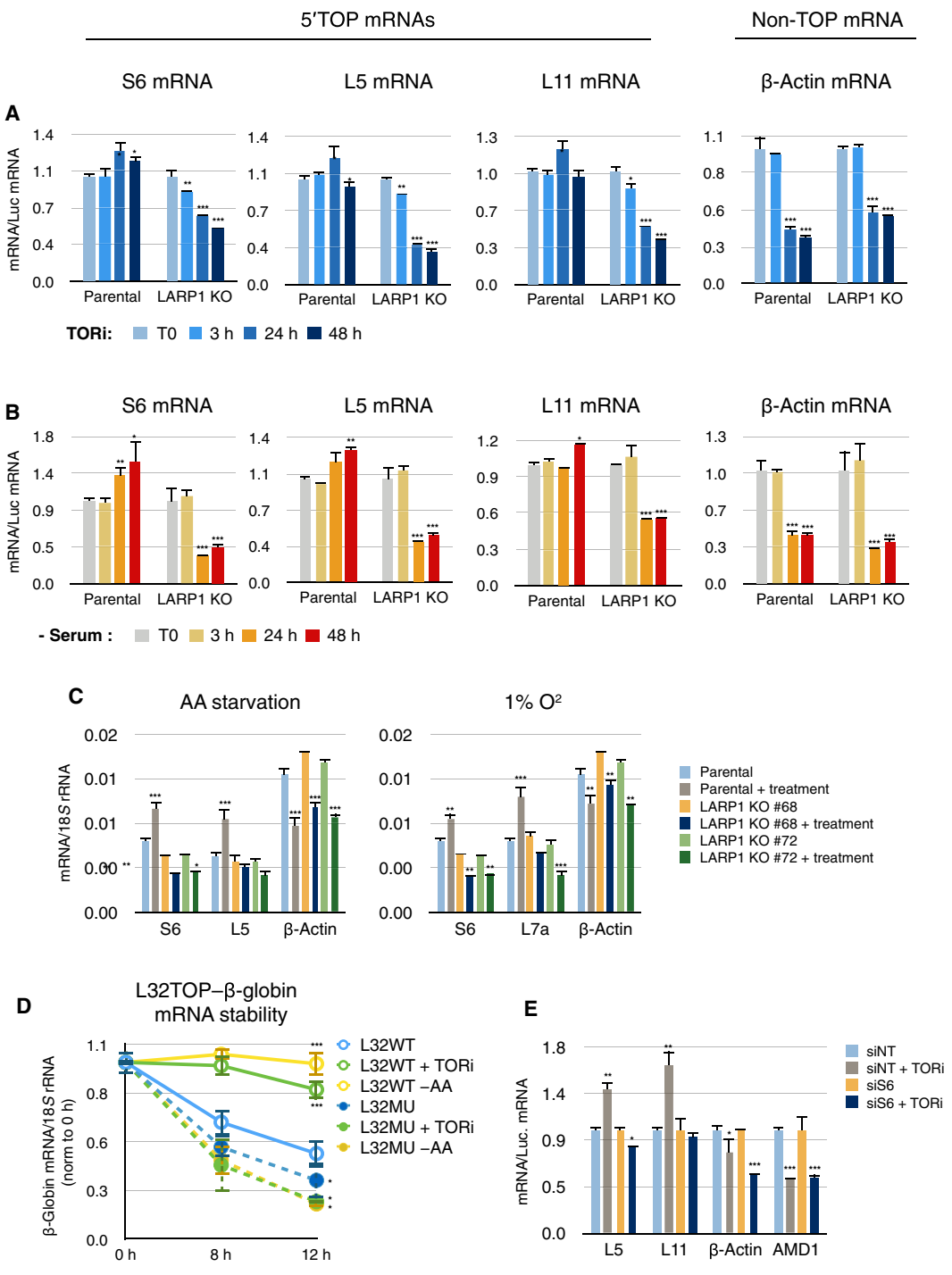

Fig. 1. Chronic mTOR inhibition increases 5′TOP mRNA stability and reduces non-TOP mRNAs levels. (**A**) HCT116 parental cells or LARP1 KO cells (clone #72) were treated with TAK228 (TORi) at 250 nM, collected at the indicated time points after treatment, counted, and spiked with a proportional amount of exogenous luciferase mRNA (see Methods). Reverse transcriptase polymerase chain reaction (RT-qPCR) was carried out to measure the levels of (RP) S6, L5, L11, and β-actin mRNAs per cell. Data are means ± SEM ($n = 3$). *$P < 0.01$, **$P < 0.001$, and ***$P < 0.0001$ by two-way analysis of variance (ANOVA) multiple comparison test with respect to time 0 (T0). (**B**) Time course analysis of serum deprivation on parental and LARP1 KO HCT116 cells was analyzed as in (A). (**C**) Parental or LARP1 KO cells (clones #68 and #72) were deprived of amino acids (left) or cultured in limiting oxygen for 20 hours (right). Then, total RNAs were analyzed by RT-qPCR analysis. (**D**) Determination of wild type (WT)–RPL32–(solid lines) and MU-RPL32–β-globin (dashed lines) mRNAs' stability in normal growing condition or upon TAK228 treatment (TORi) or amino acid deprivation (–AA) as previously described (*22*). All time points were normalized to time 0 of doxycycline deprival. $P < 0.05$ by Student's two-tailed t test. Means and SEM are shown ($n = 3$). (**E**) HCT116 transfected with an small interfering RNAs (siRNA) against RPS6 (siS6) or with a nontargeting control sequence (siNT) for 24 hours was cultured in control medium or medium supplemented with 250 nM TAK228 (TORi) for additional 24 hours. RP mRNAs and non-TOP mRNAs were assayed by RT-qPCR on total RNAs.

40S-LARP1 complex protects 5′TOP mRNAs in a translationally inactive state upon prolonged mTOR inhibition to escape the effects of ribophagy

The observation that upon chronic mTOR inhibition, both LARP1 and the 40*S* ribosomes are necessary for the preservation of 5′TOP transcripts suggested that it was mediated by the 40*S*-LARP1 complex. As in LARP1 KO cells, the amount of RP mRNAs, such as RPL5 mRNA, co-sedimenting with non-polysomal fractions is markedly reduced when compared to parental cells (fig. S2A), we hypothesized that the impairment in preserving 5′TOP mRNAs upon mTOR inhibition was due to the inability of those transcripts to associate with 40*S* ribosomes as a consequence of the loss of LARP1. Polysome profile analysis of HCT116 cells following 3 hours of TAK228 treatment also revealed a rapid redistribution of RPS6 mRNA (Fig. 2A, left) and LARP1 protein (Fig. 2B) to the 40*S* and 80*S* fractions at the expenses of the polysomal fractions, and their levels were maintained or slightly increased at 24 hours [Fig. 2, A (left) and B] and 48 hours of treatment (fig. S2B, left). In contrast, β-actin mRNA, which, after 3 hours of TAK228 treatment, remained associated with the polysomes with no apparent changes in its distribution, displayed a remarkable decrease in its levels at 24 hours (Fig. 2A, right) and at 48 hours after TAK228 treatment (fig. S2B, right). These results are consistent with the drop in total β-actin mRNA levels (Fig. 1A) and with a decrease in polysome size following prolonged TAK228 treatment (Fig. 2A). In line with our hypothesis in LARP1 KO cells, the RPS6 mRNA did not accumulate in 40*S* and 80*S* fractions following TAK228 treatment over time, while its polysomal levels were progressively reduced (Fig. 2C and fig. S2C), recapitulating the trend observed for β-actin mRNA (Fig. 2A, right) and indicating that LARP1 is necessary to rapidly redirect 5′TOP mRNAs to nonpolysomal 40*S* and 80*S* ribosomes. It should be noted that the effects of prolonged mTOR inhibition are not limited to tumoral contexts, as they are also observed in wild-type (WT) mouse embryo fibroblast (MEF) (Fig. 2D and fig. S2D).

Under the experimental conditions used above, the redistribution of 5′TOP-LARP1 upon mTOR inhibition occurred to a variable extent to either nonpolysomal 40*S* or 80*S* ribosomes. Suppressing the synthesis of the 40*S* subunit hampered the accumulation of RPL5 mRNA and LARP1 protein not only in the free 40*S* fraction but also in the 80*S* fraction (Fig. 2E), indicating that the accumulation of LARP1 and 5′TOP mRNAs with the 80*S* monosomes depends on the 40*S* ribosomes.

To test whether the 5′TOP mRNAs associated with 80*S* monosomes upon TOR inhibition were translationally inactive, we acutely treated cells with puromycin, which leads to a premature termination of translating ribosomes, on TAK228-administered cells and verified no reduction in the accumulation of RP mRNAs cosedimenting with 80*S* fraction, indicating that 5′TOP mRNAs associated with 80*S* ribosomes are translationally inactive (Fig. 2F and fig. S2E).

Upon mTOR inhibition, the redistribution of 5′TOPs from polysomes to nonpolysomes by 40*S*-LARP1 complex is an early event that takes place before major changes are observed in global polysome size or in the association of non-TOP mRNAs with polysomes (Fig. 2A). As RP mRNAs in LARP1 KO cells remain on polysomes after TAK228 treatment, we reasoned that they are exposed to global polysome changes as demonstrated by their reduced levels at 24 and 48 hours (Fig. 2, A and C, and fig. S2C). In this respect, ribophagy is a consequence of prolonged mTOR inhibition that stimulates the selective degradation of ribosomes (*5*), which, by sucrose fractionation, appears to occur at the expense of the polysomal population (Fig. 2A), and that could be accountable for the reduction of non-TOP mRNAs. Consistent with this hypothesis in autophagy-insensitive *Atg7*$^{-/-}$ MEFs, the total levels of the non-TOP mRNA β-actin upon TAK228 administration were rescued when compared to WT MEFs (Fig. 3, A and B). In LARP1 KO HCT116 cells, in which 5′TOP mRNAs are not stabilized by the 40*S*-LARP1 complex, the knockdown of the ribophagy effector NUFIP1 (nuclear FMR1 interacting protein 1) rescued not only the non-TOP levels but also the RP mRNAs, both upon pharmacological mTOR inhibition or upon serum deprivation, indicating that the 40*S*-LARP1 complex protects 5′TOP mRNAs from ribophagy (Fig. 3, C and D). Of note, measuring the distribution of those transcripts on sucrose gradient confirmed that the rescue observed by NUFIP1 knockdown occurred on the polysomal fractions (Fig. 3E). Overall these observations demonstrate that, upon mTOR inhibition, the 40*S*-LARP1 complex quickly redistributes the 5′TOP mRNAs with nonpolysomes to escape ribophagy-dependent degradation and to preserve them over time in a translationally inactive state, while non-TOP mRNAs are progressively destabilized paralleling the reduction in polysomes consequent to prolonged mTOR inhibition, providing a mechanistic rationale to explain the differential behaviors of 5′TOP and non-TOP mRNAs.

Overriding mTOR inhibition upon amino acid or serum deprivation bypasses LARP1-5′TOP redistribution with nontranslating ribosomes

Previous studies have demonstrated that acute amino acid deprivation resets the translational output of 5′TOP mRNAs and that specific translational factors (TFs) other than LARP1 are involved in inhibiting 5′TOP translation (*31*). As we observed that prolonged amino acid deprivation phenocopies the effects of pharmacological mTOR inhibition on total RNA levels in a LARP1-dependent manner (Fig. 1, C and D), we sought to investigate whether the mechanism(s) underpinning amino acid deprivation is also controlled by the 40*S*-LARP1 complex. We subjected parental and LARP1 KO HCT116 cells to amino acid deprivation (−AA) for 16 hours and then resolved the cellular ribosomes on sucrose gradients. As for pharmacological mTOR inhibition, 16 hours of amino acid starvation led to the accumulation of RPS6 mRNA and LARP1 protein with 40*S* and 80*S* fractions but, in the absence of LARP1 RPS6 mRNA, remained on polysomes and was found reduced in levels reflecting the drop in polysome size (Fig. 4, A and B), arguing that amino acid limitation is also inducing the formation of 40*S*-LARP1-5′TOP complex to preserve 5′TOP mRNAs in a translationally inactive state. A similar observation was obtained when we exposed parental and LARP1 KO HCT116 cells to 20 hours of serum deprivation (Fig. 4, C and D).

To confirm that mTOR inhibition following nutrient limitation (fig. S1H) is driving the protection of 5′TOP mRNAs by the 40*S*-LARP1 complex, we made use of *Tsc2*$^{-/-}$ MEFs, which are desensitized for mTOR inhibition in response to serum and amino acid deprivation (*32*). As anticipated, the *Tsc2* KO mutation overrides the mTOR inhibition after serum starvation as observed in WT MEFs (fig. S3A). Under these conditions, sucrose gradient fractionation of polysomal lysates derived from WT MEFs confirmed that 5′TOP mRNAs and LARP1 protein cosedimented with the 40*S* and 80*S* ribosomes [Fig. 4, E (left) and F, and fig. S3B (left)], as observed in HCT116 (Fig. 4, C and D). However, this redistribution was hampered in *Tsc2*$^{-/-}$ MEFs, maintaining 5′TOP mRNAs on

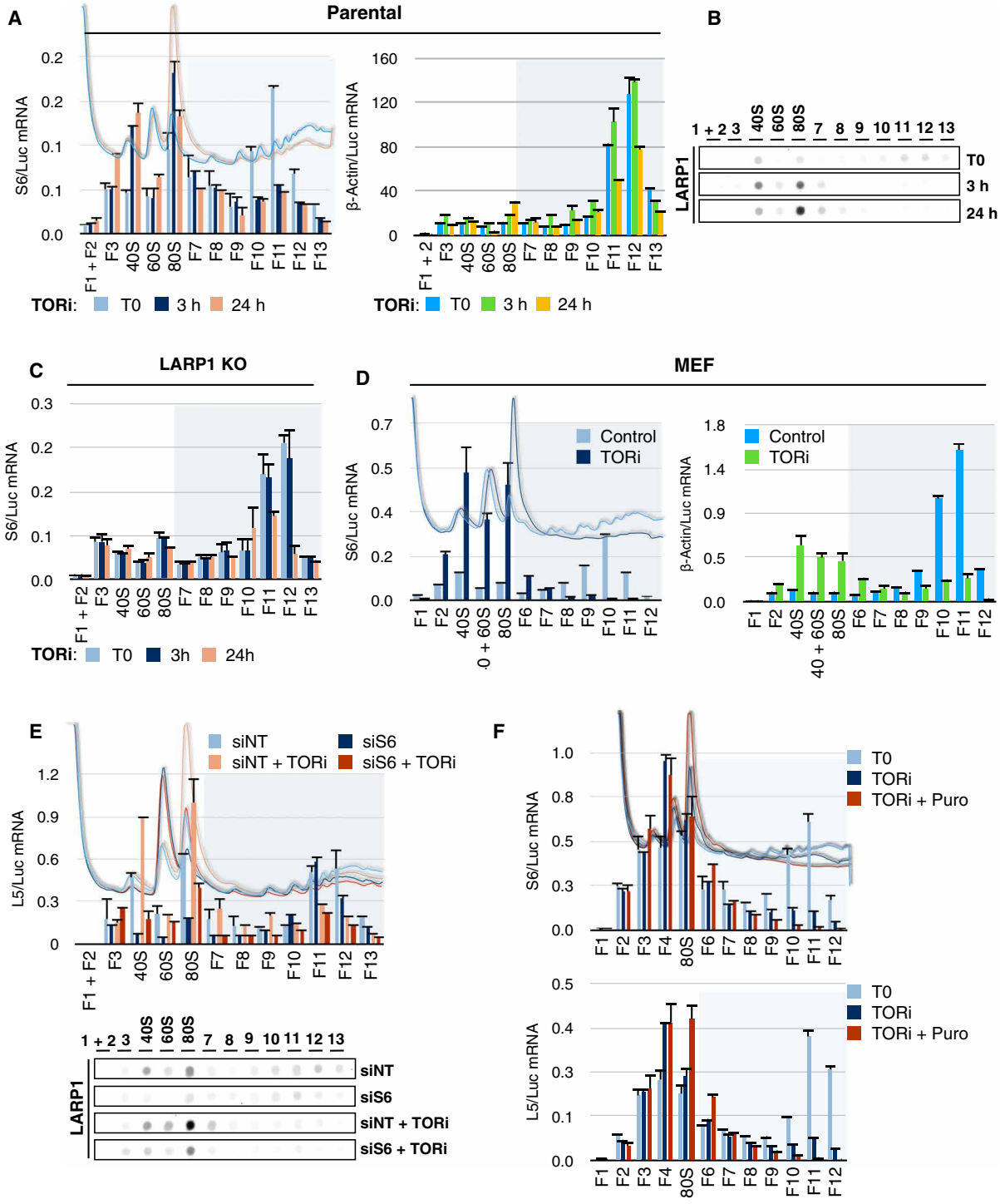

Fig. 2. 40*S*-LARP1 complex protects 5′TOP mRNAs in a translationally inactive state upon prolonged mTOR inhibition. Polysome profile analysis of HCT116 parental (**A**) and LARP1 KO (**C**) cells treated with TAK228 (TORi) at 0, 3, and 24 hours. S6 and β-actin mRNAs distributions across the gradient were evaluated in each fraction by real-time qPCR as described in Methods. Light gray area marks polysomes. (**B**) Protein analysis from 20% volume of sucrose gradient fractions as in Fig. 2A was subjected to dot blot analysis with an anti-LARP1 antibody. (**D**) Polysome profile analysis of MEFs cultured with normal growing medium or medium supplemented with TAK228 (TORi) for 24 hours. RPS6 (left) and β-actin (right) mRNAs were monitored across the gradient as in Fig. 2A. (**E**) Polysomal lysates from HCT116 parental cells treated as in Fig. 1E were resolved by sucrose gradient fractionation, and RPL5 mRNA distribution was determined by RT-qPCR (top). Twenty percent of the fraction volumes from a replicate experiment were assayed by dot blot for LARP1 protein distribution (bottom). (**F**) HCT116 parental cells cultured in normal growing medium or medium supplemented with TAK228 (TORi) for 48 hours without or with puromycin pretreatment for the past 15 min. RPS6 and RPL5 mRNAs were measured (top and middle panels).

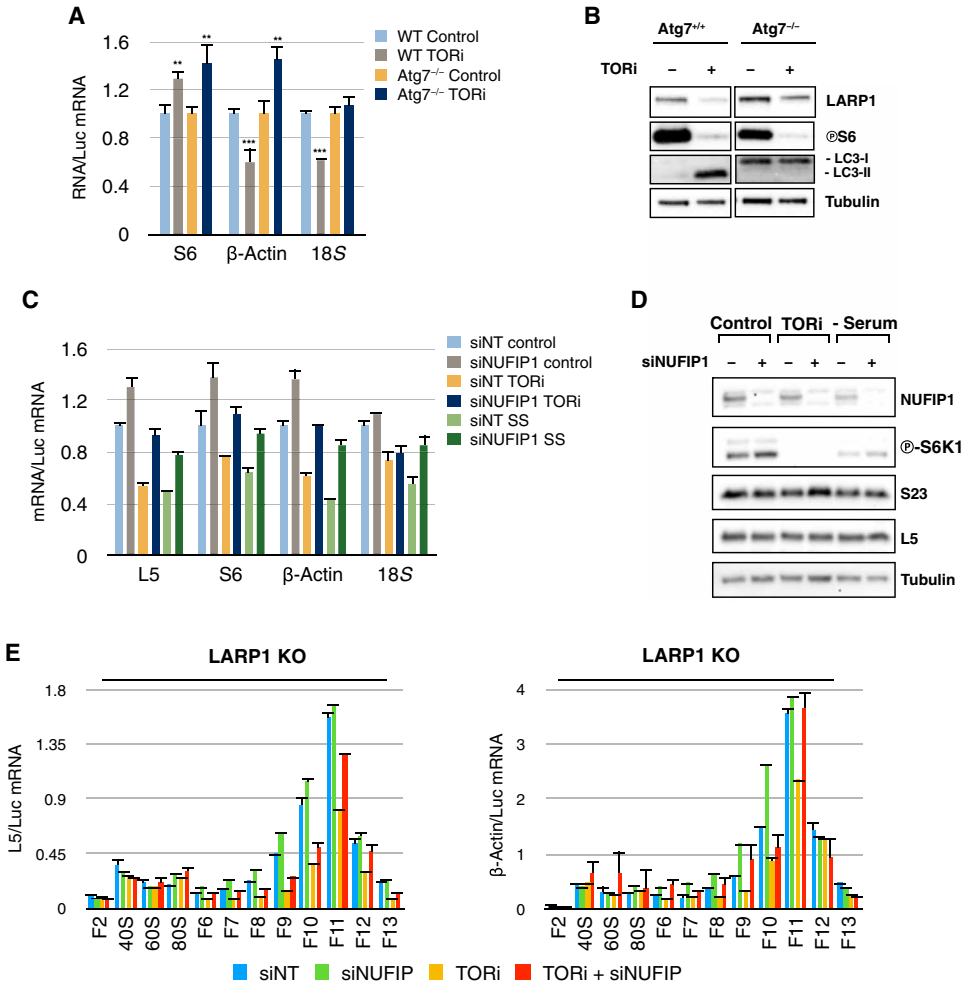

Fig. 3. Redistribution of 5′TOP by 40*S*-LARP1 with nonpolysomes after mTOR inhibition is critical to escape the effects of ribophagy. (**A**) Total RNA extracted from WT or *Atg7*$^{-/-}$ MEFs cultured in the absence or presence of TAK228 (TORi) for 24 hours were assayed by RT-qPCR. $^{**}P < 0.01$ and $^{***}P < 0.001$. (**B**) Total cellular lysates from (A) were resolved by Western blot and probed with the indicated antibodies. (**C** to **E**) HCT116 LARP1 KO cells were transfected with an siRNA against NUFIP1 (siNUFIP1) or with a nontargeting control sequence (siNT). The day after transfection cells were treated for additional 24 hours with TAK228 (TORi), deprived of serum (SS), or maintained in normal growing medium (control). Total RNA was assayed by RT-qPCR analysis to determine the levels of RPL5, RPS6, β-actin, and 18*S* rRNA (C) and total protein levels of NUFIP1, phospho-S6K1 (T389), RPS23, RPL5, and α-tubulin were determined (D). Polysomal lysates obtained from the same samples from (C) and (D) were subjected to sucrose gradient ultracentrifugation, and each fraction was monitored by RT-qPCR for RPL5 and β-actin mRNA levels (E).

polysomes and leading to their destabilization [Fig. 4, E (right) and F, and fig. S3B (right)] as observed for β-actin mRNA in both genetic contexts (fig. S3C). Similar to serum starvation, upon amino acids deprivation, RP mRNAs and LARP1 protein accumulated in 40*S*-containing fractions in the nonpolysomal part of the gradient of WT MEFs lysates. However, in *Tsc2*$^{-/-}$ MEFs, where amino acid deprivation does not inactivate mTOR signaling as in WT MEFs (fig. S3D) (*32*), RP mRNAs and LARP1 protein did not redistribute with nonpolysomes and were decreased in their levels (Fig. 4, G and H) as observed for β-actin mRNA in both genetic contexts (fig. S3, E and F). Consistent with an inhibition of mTORC1 operated by nutrients deprivation and in line with the data obtained in a hyperactive mTORC1 genetic context (Fig. 4, E to H) and by the rapamycin treatment (fig. S1G), genetic ablation of RAPTOR, which selectively restrains the mTOR complex 1 signaling (fig. S3G), recapitulated the nonpolysomal accumulation of LARP1 triggered by mTOR pharmacological inhibition (fig. S3H). In summary, mTOR inhibition as a consequence of amino acid or serum deprivation stabilizes 5′TOP mRNAs in a translationally inactive state by means of LARP1-5′TOP redistribution with the 40*S* subunit, reproducing the effect of pharmacological mTOR inhibition.

40*S*-LARP1 complex reprograms the cellular translatome upon chronic mTOR inhibition

mTOR is a pivotal metabolic effector in the cell, and negative growth or negative proliferative signals are designed to converge on mTOR inhibition to prepare the cell to face an upcoming shortage of nutrients. The evidence that, in these conditions, the 40*S*-LARP1 complex is protecting a discrete population of transcripts and maintains them selectively associated with the translational machinery suggested that the complex was acting to reprogram the translational landscape. This raises the question of which mRNAs are selectively maintained translationally inactive within the translatome by this mechanism. To address this question, we exposed HCT116 parental and

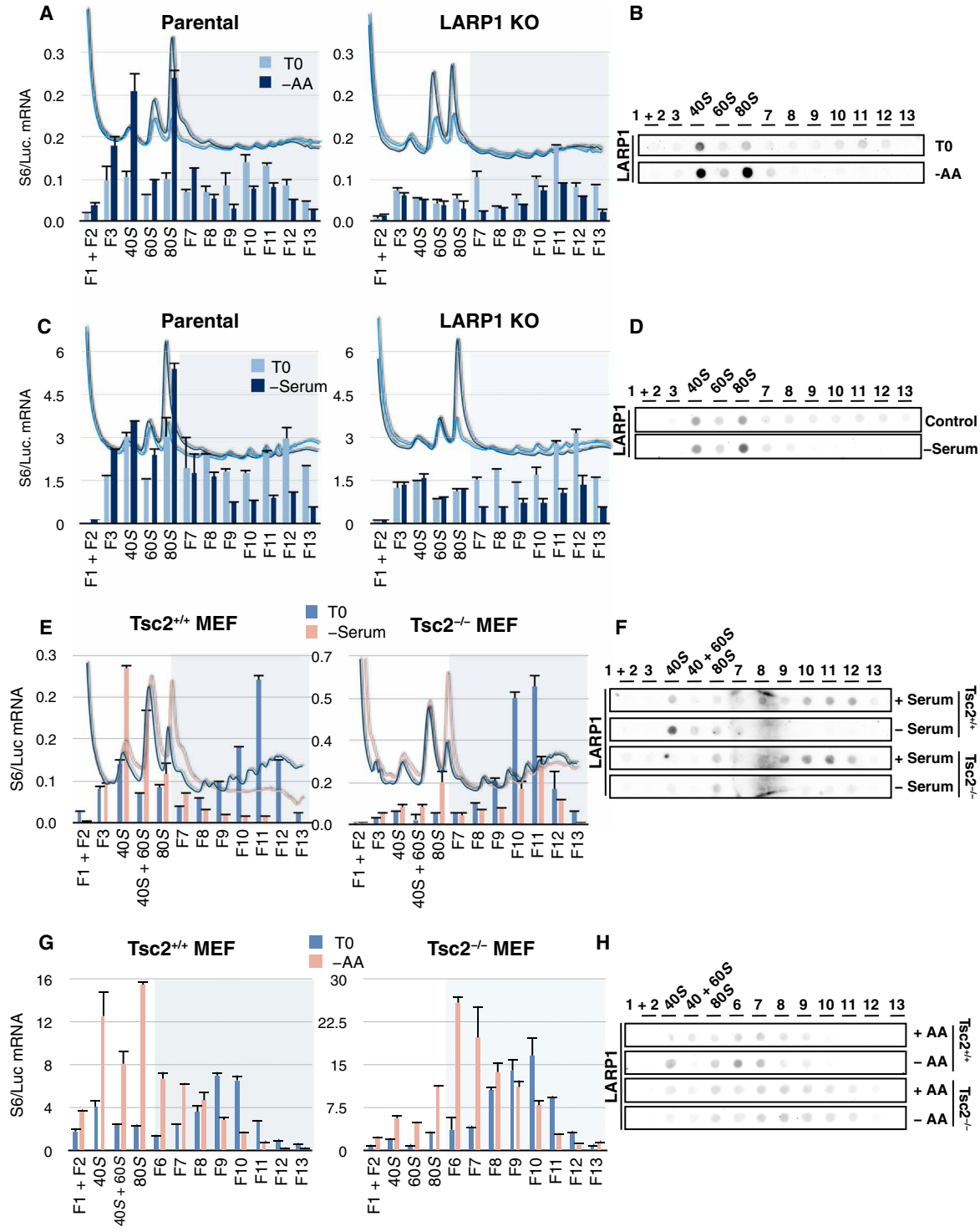

Fig. 4. Overriding mTOR inhibition upon amino acid or serum deprivation bypasses LARP1–5′TOP redistribution with non-translating ribosomes. HCT116 parental and LARP1 KO control cells or cells deprived of amino acids (–AA) for 16 hours were analyzed by polysome profile. (**A**) RPS6 mRNA distribution across the gradient was determined and (**B**) LARP1 protein was measured in each fraction from parental cells. (**C** and **D**) HCT116 cells were analyzed as in (A) and (B) upon serum deprivation for 20 hours. (**E**) Tsc2 WT or Tsc2$^{-/-}$ MEFs were cultured in normal growing medium or medium deprived of serum for 20 hours. Polysomal lysates were resolved by polysome profiling. RPS6 mRNA distribution was assayed, and (**F**) LARP1 protein distribution was measured by dot blot analysis. (**G**) WT or Tsc2$^{-/-}$ MEFs were cultured with normal growing medium or medium deprived of amino acids for 6 hours, cellular lysates were analyzed by polysome profiling, and RPS6 mRNA levels were measured across the gradient. (**H**) 20% of fraction volume from Fig. 4G were probed for LARP1 protein distribution.

LARP1 KO cells to TAK228 for 48 hours and resolved the mRNPs (messenger ribonucleoproteins) by polysome profiling (Fig. 4A and fig. S4A). We then purified the RNA from the pooled fractions spanning from 40*S* to the 80*S* ribosomal peaks from both cell types treated with TAK228 and spiked with a library of exogenous mRNAs for normalization purposes and then subjected the corresponding libraries to RNA-seq analysis as depicted in Fig. 5B. Differential analysis upon mTOR inhibition revealed a marked enrichment of transcripts accumulated with nonpolysomes as a function of LARP1 expression that passed the filter of absolute log 2 fold change of ≥ 1 and $-\log_{10}$ adjusted *P* value of ≥ 2 (Fig. 5C, left, and tables S1 and S2). As anticipated, almost all RP mRNAs (80) where found enriched by LARP1 expression upon mTOR long-term pharmacological inhibition (Fig. 5C, middle) as well as many elongation and initiation TFs, including 12 subunits forming the eIF3 (eukaryotic initiation factor 3) complex (Fig. 5C, right, and fig. S4C). In addition to ribosome and translational components, many ribosome biogenesis assisting factors—including RNA pol I subunits, snoRNA host genes (SNHGs) involved in rRNA editing, and nascent polypeptide chaperoning factors—were also found enriched, indicating that upon mTOR inhibition, LARP1 preserves the protein synthetic potential in the form of stored mRNA (tables S1 and S2). Other transcripts whose cognate proteins are involved in metabolic processes including nucleotide biosynthesis [IMPDH2 (inosine monophosphate dehydrogenase 2) and NME2 (nucleotide diphosphate kinase 2)] or components of the mitochondrial inner and outer membrane, oxidative phosphorylation [COXs (cytochrome C oxidase subunits), NDUFs (NADH:ubiquinone oxidoreductase subunits), ATP5s (ATP synthase F1 and membrane subunits), and UQCRs (ubiquinol-cytochrome C reductase)], glycolysis [glyceraldehyde-3-phosphate dehydrogenase (GAPDH), ALDOA (aldolase A), and LDHB (lactate dehydrogenase B)], and pentose phosphate pathway (TKT) clustered among the 500 most enriched transcripts, as revealed by Gene Ontology analysis (Fig. 5D and table S2).

This notable overlap with the repertoire of mRNAs found in the 40-LARP1 complex (table S2) suggested that the transcripts enriched by LARP1 expression with nonpolysomes, which are not RPs or TFs, could also be 5′TOP mRNAs. In our recent study (*22*), we verified those transcripts isolated in the 40*S*-LARP1 complex to fall in the 5′TOP family of mRNAs by querying the TSS repository database (https://dbtss.hgc.jp) generated from total RNAs from different cell lines and tissues. There we found that most of the RP genes has a unique delimited genomic region where the RNA polymerase II swings around a predominant TSS that generates 5′TOP transcripts we have termed "pure TOPs," whereas in many cases of non-RP mRNAs, more than one delimited genomic region is used by RNA polymerase II to generate different 5′ untranslated region (5′UTR) transcript isoforms with at least one 5′TOP, here termed "nonpure TOPs" (fig. S4, D and E). To verify whether LARP1 selectively protected 5′TOP transcript isoforms upon mTOR inhibition, we processed the parental RNAs, the same used for RNA-seq (Fig. 5C), to reveal the TSSs. The RNA samples were treated with alkalyne phosphatase to dephosphorylate spurious 5′ termini derived from RNA breakpoints occurring during the RNA extraction and/or manipulation. This step was followed by TAP (tobacco acid pyrophosphatase) enzymatic treatment, which mediates RNA decapping, exposing the genuine TSSs phosphorylated at the 5′, making them amenable to ligation with an exogenous RNA oligonucleotide sequence (Fig. 5B). RNA-seq libraries were prepared and sequenced, and TSS reads were identified as described in experimental procedures. As expected, TSSs of pure 5′TOP mRNAs such as RPL11, RPS6, and EEF2 confirmed the canonical transcript isoforms described in database of transcriptional start sites (dbTSS) (fig. S4F). Representative results are shown for GAPDH and IMPDH2 mRNAs whose TSSs in dbTSS database cluster in two regions generating non-TOP and 5′TOP 5′UTR isoforms, respectively (fig. S4, D and E). GAPDH isoforms protected by LARP1 in the non-polysomal pooled fraction following long-term mTOR inhibition almost exclusively contained a 5′TOP at their TSS, which was also the case for other representative mRNAs such as BTF3 (basic transcription factor 3), IMPDH2, SLC25A3 (solute carrier family 25 member 3), HSPA8 [heat shock protein family A (Hsp70) member 8], and ATP5E (ATP5F1E) (Fig. 5E and table S2). Reverse transcriptase polymerase chain reaction (RT-qPCR) analysis on polyadenylated [poly $(A)^+$] RNAs from nonpolysomal RNAs obtained from Fig. 5C confirmed that, in addition to RP mRNAs, also nonpure TOPs such as GAPDH mRNA accumulate in nonpolysomal fraction in a LARP1-dependent manner (Fig. 5F). In agreement with the 5′TOP motif being the molecular determinant of transcript protection by the 40*S*-LARP1 complex, the TSS analysis of a number of representative transcripts obtained from the list of most expressed mRNAs not enriched by TORi (TOR inhibition) in parental versus LARP1 KO cells (table S2, Tab non-TOPs) confirmed the presence of a non-TOP TSS pattern, having all transcript isoforms a TSS starting with a nucleotide other than cytosine followed by a C/T sequence (fig. S4G). Overall, these results indicate that mTOR inhibition operates a translational reprogramming by means of LARP1 and 40*S* native ribosomes selectively maintaining 5′TOP mRNAs in a stable translationally inactive state.

Reactivation of mTOR signaling acutely reconstitutes the ribosome biogenesis and protein synthetic capacity of the cell in a LARP1-dependent manner

Prolonged mTOR inhibition reshapes the repertoire of transcripts associated with the translational machinery by means of LARP1 and the native 40*S* subunit. The evidence that the LARP1-protected translatome is maintained in a translationally inactive state suggests that the cell retains, in a "loaded gun" fashion, the ability to rapidly translate those transcripts upon demand. As mTOR signaling is sustained by positive anabolic stimuli, we reasoned that reactivating mTOR should rapidly trigger the selective translation of the LARP1-protected translatome. To verify this hypothesis, HCT116 parental and LARP1 KO cells were harvested before treatment ($t = 0$), after 48 hours of exposure to TAK228 (TORi), and at 48 hours with TAK228 followed by the removal of mTOR inhibitor for additional 75 min (washout). Removal of TAK228 was confirmed by the reactivation of the mTOR signaling in both cell types (fig. S5A). In parallel, we resolved the polysomal lysates obtained under the same experimental conditions by sucrose gradient fractionation and measured the engagement in translation of a number of mRNAs. Strikingly, the amount of RPS6 and RPL5 mRNAs accumulated in the 40*S* /80*S* fractions upon prolonged mTOR inhibition in parental cells rapidly redistributed on polysomes after drug removal, indicating a rapid engagement in translation of these transcripts (Fig. 6A, top panels). A non-TOP mRNA such as β-actin, which did not accumulate on nonpolysomes after prolonged mTOR inhibition, was not mostly affected by TAK228 removal (fig. S5B). The same evidence observed for β-actin mRNA was also observed for RPS6 and RPL5 mRNAs in LARP1 KO cells, which lacked the ability after TAK228 treatment to preserve 5′TOP mRNAs on nonpolysomes (Fig. 6A,

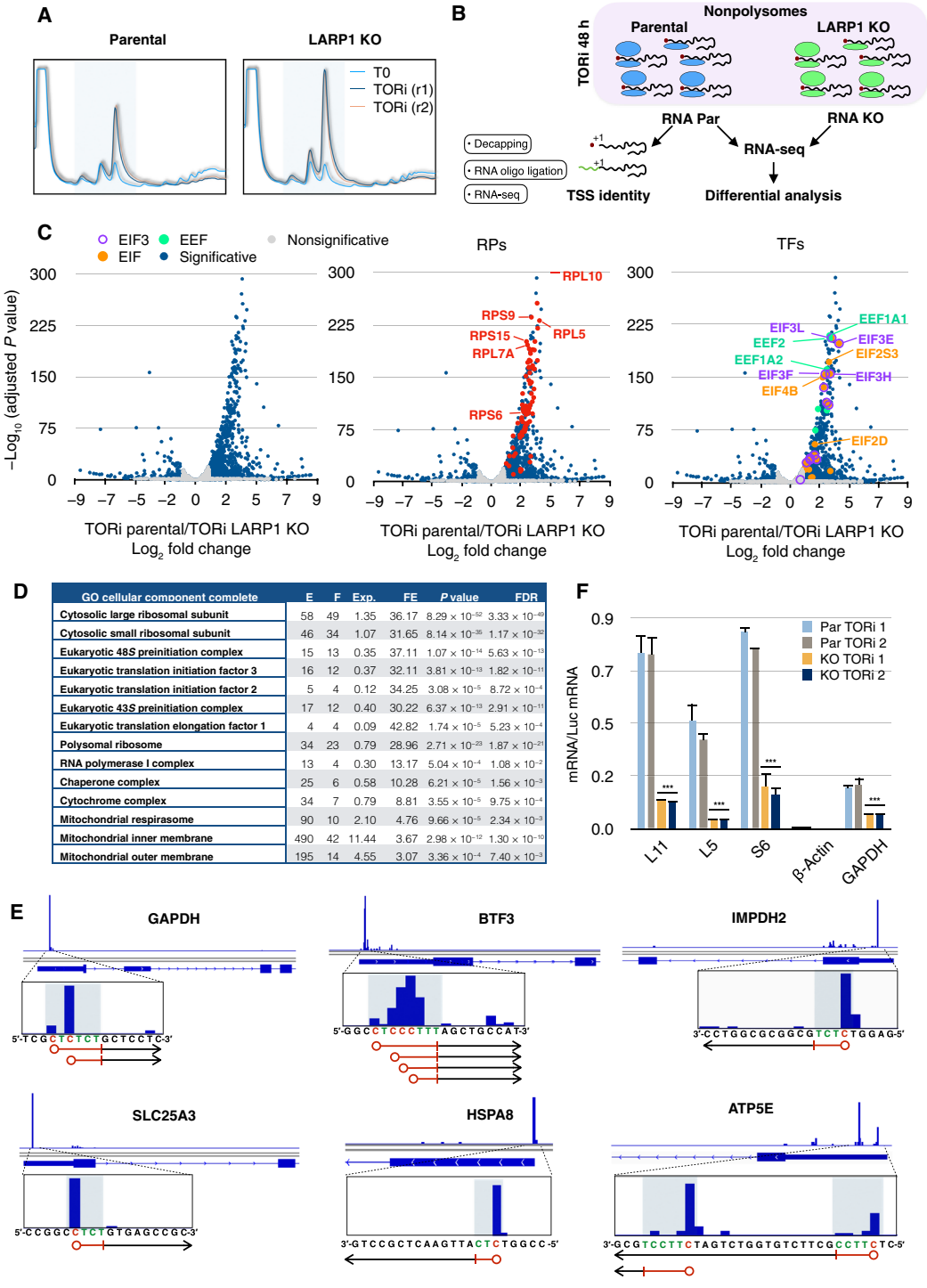

GO cellular component complete	E	F	Exp.	FE	*P* value	FDR
Cytosolic large ribosomal subunit	58	49	1.35	36.17	8.29×10^{-52}	3.33×10^{-49}
Cytosolic small ribosomal subunit	46	34	1.07	31.65	8.14×10^{-35}	1.17×10^{-32}
Eukaryotic 48*S* preinitiation complex	15	13	0.35	37.11	1.07×10^{-14}	5.63×10^{-13}
Eukaryotic translation initiation factor 3	16	12	0.37	32.11	3.81×10^{-13}	1.82×10^{-11}
Eukaryotic translation initiation factor 2	5	4	0.12	34.25	3.08×10^{-5}	8.72×10^{-4}
Eukaryotic 43*S* preinitiation complex	17	12	0.40	30.22	6.37×10^{-13}	2.91×10^{-11}
Eukaryotic translation elongation factor 1	4	4	0.09	42.82	1.74×10^{-5}	5.23×10^{-4}
Polysomal ribosome	34	23	0.79	28.96	2.71×10^{-23}	1.87×10^{-21}
RNA polymerase I complex	13	4	0.30	13.17	5.04×10^{-4}	1.08×10^{-2}
Chaperone complex	25	6	0.58	10.28	6.21×10^{-5}	1.56×10^{-3}
Cytochrome complex	34	7	0.79	8.81	3.55×10^{-5}	9.75×10^{-4}
Mitochondrial respirasome	90	10	2.10	4.76	9.66×10^{-5}	2.34×10^{-3}
Mitochondrial inner membrane	490	42	11.44	3.67	2.98×10^{-12}	1.30×10^{-10}
Mitochondrial outer membrane	195	14	4.55	3.07	3.36×10^{-4}	7.40×10^{-3}

Fig. 5. 40*S*-LARP1 complex reprograms the cellular translatome upon chronic mTOR inhibition. (**A**) Sucrose fractionation of polysomal lysates from parental or LARP1 KO control cells or cells treated with TAK228 for 48 hours (TORi replicates r1 and r2). Fractions from 40*S* to 80*S* peaks (light gray area) were pooled. (**B**) Scheme of the analysis performed on nonpolysomal RNAs extracted from pools obtained in Fig. 4A (see Methods). (**C**) Differential analysis of nonpolysomal transcripts upon TOR inhibition of parental/LARP1 KO cells (left) of which RP mRNAs are labeled in red (middle), and TFs are reported in green [eEFs (eEFs eukaryotic elongation factors)], orange [eIFs (eukaryotic initiation factors)], or circled in purple (eIF3s) (right). (**D**) Gene Ontology analysis of 485 mRNAs was identified from (C) and filtered by $-\log_{10} Q$ value of ≥15 and log 2 fold change of ≥1. *E* = number of transcripts belonging to the biological process. *F* = number of transcripts found in the filtered dataset from (C). FE, fold enrichment; FDR, false discovery rate. (**E**) TSS sequencing of representative transcripts belonging to different cellular processes [shown in (D)] accumulated with nonpolysomes in parental cells upon TOR inhibition as described in (B). Bars aligning with the first exon of GAPDH, BTF3, IMPDH2, SLC25A3, HSPA8, and ATP5E define the corresponding TSS(s). Bar height is proportional to the number of reads. Inlet zoom in of the TSS regions reveals the corresponding sequence, with the cytosine(s) in red marking the TSS(s) followed by a green C/T sequence, which defines the TOP motif. (**F**) RT-qPCR of polyA$^+$ mRNAs isolated from RNAs used in (C). ***$P < 0.0001$.

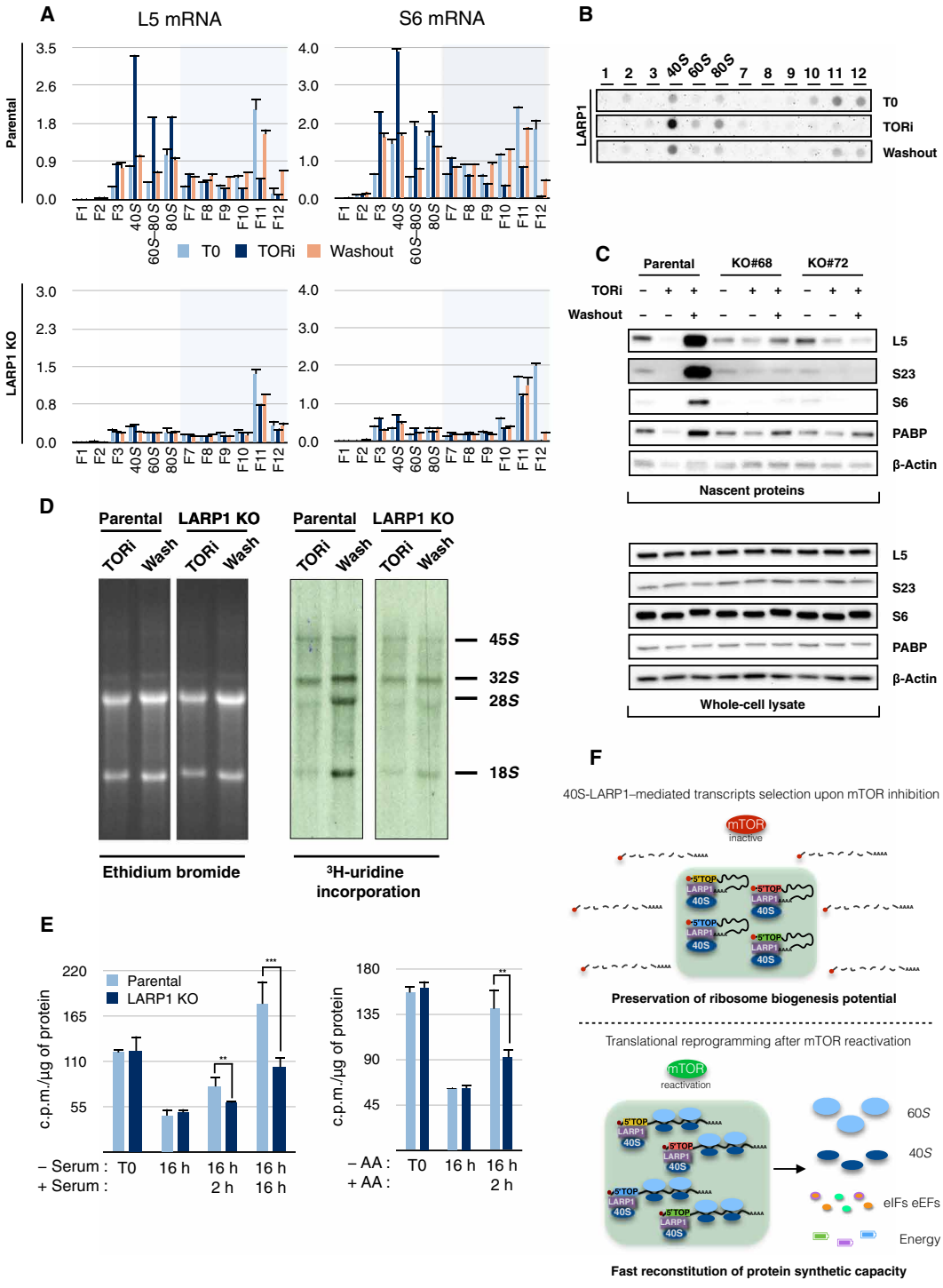

Fig. 6. Reactivation of mTOR signaling acutely reconstitutes the ribosome biogenesis and protein synthetic capacity of the cell in an LARP1-dependent manner. (**A**) Polysome profile analysis of parental (top panels) and LARP1 KO cells (bottom panels) at the time of treatment (T0), treated for 48 hours with TAK228 (TORi) or 48 hours of TAK228 treatment followed by 75 min of drug removal (washout). RPS6 and RPL5 transcripts were measured in each fraction. (**B**) Dot blot analysis from Fig. 5A probed with an LARP1 antibody. (**B**) Cells treated as in Fig. 5A with the modification of a 2-hour pulse with the methionine analog AHA for the last 2 hours of treatment. Nascent proteins (top) were detected by Click-iT chemistry as previously described (*22*). In parallel, total proteins (bottom) were analyzed. (**D**) Parental and LARP1 KO cells were cultured as in Fig. 5C, with the modification of pulsing them with ^{3}H-uridine for the past 2 hours of treatment. Nascent rRNA was detected by Northern blot and autoradiography. (**E**) Cells cultured for 16 hours in medium deprived of serum (left) or amino acids (right). Serum or amino acids were them replenished for 2 and/or 16 hours. In the past 30 min, cells were pulsed with ^{3}H-leucine to measure the rate of protein synthesis, and leucine incorporation per microgram of total protein was calculated in each condition. c.p.m., counts per minute. (**F**) Sketch representing the working model of 40*S*-LARP1 complex protecting 5′TOP mRNAs with the translational machinery upon mTOR inhibition. Immediate translation of 5′TOP mRNAs protected by 40*S*-LARP1 occurs when mTOR signaling is reactivated by an anabolic signal.

bottom panels). In agreement with the working model of LARP1 controlling the selective preservation/translational reengagement of 5′TOP mRNAs, the pattern of LARP1 protein sedimentation overlapped with the RP mRNAs redistribution after TAK228 removal (Fig. 6B). GAPDH, ATP5PO, and COX4I1 mRNAs, whose 5′TOP isoforms were found protected by the 40*S*-LARP1 complex (table S2 and Fig. 5E), also recapitulated the RP mRNA distribution upon mTOR inhibition/reactivation in HCT116 parental cells (fig. S5C), confirming the evidences observed by RNA-seq analysis (Fig. 5E). To assess the extent of the translational activation of the 40*S*-LARP1–protected RP mRNAs in the production of their cognate proteins, we labeled nascent proteins in the same experimental setup with a methionine analog [azyde-homoalanine (AHA)] amenable for Click-iT chemistry. De novo protein analysis confirmed that the synthesis of RPs and other 5′TOP mRNAs markedly increased upon TAK228 removal only in LARP1-expressing cells (Fig. 6C). Moreover, the same approach conducted at a proteome wide level confirmed a notable correspondence between the mRNAs protected by LARP1 upon mTOR inhibition (Fig. 5C) and the newly synthesized proteins in cells after TOR inhibitor removal, with 66 RPs among the first 179 translationally unregulated proteins after TAK228 removal (table S3). As all RP mRNAs were largely found preserved by LARP1 along with ribosome biogenesis assisting factors and other components essential for ribosome biogenesis (Fig. 5C and table S2), we measured the cell capacity to produce new ribosomes after prolonged mTOR inhibition followed by its acute reactivation. As for nascent proteins, ^{3}H-uridine incorporation into nascent rRNA, particularly the mature 18*S* and 28*S* rRNAs, was up-regulated only in parental cells after drug washout (Fig. 6D), indicating that the newly synthesized RPs observed in Fig. 5C are used to rapidly generate new ribosomes and that LARP1 upon mTOR inhibition followed by reactivation is able to coordinate an entire biological process, the ribosome biogenesis. The increase in the ribosome content after mTOR reactivation along with the preservation and synthesis of TFs (Fig. 5C) suggested that the mTOR-LARP1 axis can quickly control the protein synthetic capacity of the cell when switching from opposite metabolic constraints. In a similar experimental setting as in Fig. 5 (A to D), ^{3}H-leucine incorporation into nascent proteins after prolonged serum or amino acid deprivation and followed respectively by serum or amino acid re-addition at different times revealed that parental and LARP1 KO cells, which have similar protein synthesis rates in normal growing conditions and upon prolonged serum or amino acid deprivation, are remarkably different in their capacity of reconstituting the rate of protein synthesis, with the parental cells being more proficient (Fig. 6E) and in line with the acute up-regulation of ribosome biogenesis after mTOR reactivation (Fig. 6D). In the same line, TAK228 washout, as operated in Fig. 5 (A to D), showed a similar response (fig. S5D). In summary, those findings suggest that in a low metabolic state, the mTOR-LARP1 axis preserves the cellular capacity of producing new ribosomes in the form of 40*S*-LARP1-5′TOP mRNA complexes, allowing the reestablishment of the protein synthetic capacity of the cell when an anabolic signal is received.

DISCUSSION

Chronic mTOR inhibition translationally prepares the cell to face an upcoming restrained metabolic state

Multiple pharmacologic and nutrient deprivation studies have molecularly defined the translational landscape triggered by acute mTOR inhibition (*31*, *33*, *34*). However, a number of biological contexts are emerging in which the mTOR pathway is constitutively reduced both in physiological and pathological settings, raising the question of which are the molecular consequences of chronic mTOR inhibition and their impact on the global metabolism (*4*, *15*). Sustained inhibition of mTOR signaling was shown to restrain the main biosynthetic routes that provide nucleotides (*35*, *36*), amino acids (*37*), lipids (*38*, *39*), and energy (*40*), leading to an overall reduction of the metabolic activities of the cell as also reflected by the reduced capacity to grow and proliferate (*41*). Only recently, the effect of prolonged mTOR inhibition has revealed the selective reduction of ribosome content (*5*), which we have verified (fig. S1C) at the expenses of the polysomal population (Fig. 2A and fig. S2B), potentially leading to a profound reshaping of the translational program of the cell. Consistent with these observations, after prolonged mTOR inhibition, the global protein synthesis rate was markedly reduced by more than 50% as compared to normal growing cells (Fig. 6E and fig. S5D), indicating a strong decrease in the major anabolic pathway of the cell and in agreement with the cytostatic effect exerted by mTOR inhibition (*41*). Despite the absence of LARP1 having a significant effect in reshaping the representation of the transcriptome (Fig. 5C), its loss does not alter the amplitude of the protein synthesis rate reduction in response to mTOR inhibition (Fig. 6E and fig. S5D), suggesting that the formation of 40*S*-LARP1-5′TOP complex in response to mTOR inhibition accounts for the preservation of the genetic information conveyed by 5′TOP transcripts in a translationally inactive state, thus preparing the cell to face an upcoming poor anabolic state.

Translational selection operated by mTOR-LARP1-5′TOP axis reprograms the cellular translatome based on the cis architecture of the transcriptome

Acute inhibition of mTOR by rapamycin drives the formation of 40*S*-LARP1-5′TOP mRNA complex (*22*). We have verified that this ternary interaction stabilizes 5′TOP transcripts upon prolonged exposure to mTOR inhibitory stimuli, which is both LARP1 and 40*S* ribosome dependent (Figs. 1, A to E, and 2, A and E). Under the same circumstances, LARP1 protects RPS6, RPL5, RPL11, and other 5′TOP mRNAs (Fig. 1, A to C, and fig. S1, D to J) in a translationally inactive state (Figs. 2F and 6C) due to their rapid redistribution to the 40*S* and 80*S* ribosomes (Fig. 2A and fig. S2B) in a 40*S*-dependent manner (Fig. 2E), rescuing them from the degradation observed for non-TOP mRNAs, which remained associated with the polysomes. In support of this model, 5′TOP mRNAs remained associated with polysomes in LARP1 KO cells after acute mTOR inhibition (3 hours) encountering the same fate as non-TOP mRNAs at longer times of mTOR inhibition (Fig. 2C and fig. S2C). Strikingly, inhibiting the ribophagy pathway by NUFIP1 knockdown in LARP1 KO cells was sufficient to rescue the turnover of both non-TOP and 5′TOP mRNAs, indicating that the 40*S*-LARP1 complex acts to protect the anabolic potential of the cell in critical metabolic conditions (Fig. 3). We cannot exclude that other canonical pathways of RNA turnover are also involved in this event, such as the P-body–mediated mRNA triage, as also observed by others in the context of sodium arsenite–induced stress response (*42*).

The reduction of both rRNA and non-TOP mRNAs increases the ratio of 5′TOP mRNAs per cellular ribosome content (Fig. 1C and fig. S1, D, G, and J), thus operating a posttranscriptional selection mechanism favoring the 5′TOP mRNAs, which are found

highly represented in their association with the translational machinery (Fig. 5C). The unbiased characterization of the transcripts protected by LARP1 expression in the 40*S* to 80*S* portion of the gradients upon chronic TAK228 treatment revealed that the 500 most enriched transcripts are mostly involved in ribosome biogenesis, protein synthesis, and energy production (Fig. 5, C and D, and tables S1 and S2). The TSS analysis of the first 200 transcripts of the list allowed to determine that they are mostly 5′TOP mRNA isoforms (table S2), indicating that the mTOR-LARP1-5′TOP axis operates a translational selection mechanism, which reprograms the cellular inactive translatome based on the original cis configuration of the transcriptome. To our knowledge, this is the first evidence indicating that the transcriptome has an innate hierarchy at the translational level that can arise upon defined metabolic constraints. The transcripts belonging to the group of "nonpure" 5′TOPs such as GAPDH, IMPDH2, and ATP5E, which are characterized by a dual TSS of which one is 5′TOP (fig. S4, D and E), are markedly enriched in their 5′TOP isoforms within nonpolysomes by the mTOR-40*S*/LARP1 axis (Figs. 5D and 4F, and tables S1 and S2), in agreement with a recent report showing that a metric in the 5′TOP motif, termed TOPscore, predicts the sensitivity to mTOR inhibition (*43*). When measuring the sucrose gradient distribution of nonpure 5′TOPs, it appears evident that they accumulate with nonpolysomes upon mTOR inhibition, although to a lesser extent than pure 5′TOP mRNAs, as predicted, and are rapidly reengaged in translation after mTOR reactivation (fig. S5C). This indicates the existence of an additional layer of regulation in the translatome plasticity that is carried out by a molecular sieving of transcript isoforms. It will be of keen interest to better characterize the overall balance between the 5′TOP and the non-TOP isoforms upon mTOR inhibition and/or in specific metabolic limitation conditions.

40*S*-LARP1 complex preserves the protein synthetic capacity of the cell through a translational network

The mRNA species protected by the 40*S*-LARP1 complex upon mTOR inhibition encompass the entire set of the 40*S* and 60*S* RPs (Fig. 5C, middle) together with multiple ribosome biogenesis assisting factors such as NOP53 (NOP53 ribosome biogenesis factor), NPM1 (nucleophosmin 1), FBL (fibrillarin), and NLE1 (notchless homolog 1); the subunits composing the eIF3 complex; and many other eukaryotic initiation and elongation factors (Fig. 5C, right, and table S2), all together indicating the coordinated preservation of the ribosome biogenesis and the protein synthetic capacity of the cell. In support of this evidence, reestablishing mTOR signaling rapidly determines the translation of those transcripts protected by the 40*S*-LARP1 complex (Fig. 6, A to C), which, in turn, are assembled into new ribosomes (Fig. 6D) to stimulate the protein synthesis rate of the cell (Fig. 6E) in a LARP1-dependent manner. LARP1 by recognizing the 5′TOP motif appears to preserve the entire protein synthesis capacity first by protecting, together with the 40*S* subunit, those transcripts from degradation upon mTOR inhibition and then by coordinating the selective translation of the protected mRNAs after mTOR reactivation (Fig. 6C). In light of this model, LARP1 decodes the information retained in the 5′TOP motif that acts as a molecular determinant to coordinate an entire anabolic translational network due to the 40*S* subunit. The presence of noncoding RNAs that play a key role in rRNA modification (SNHG19, SHNG29, SNHG16, SNHG32, SNHG6, and GAS5) (*44*) also contained a 5′TOP element at their TSS (table S2), corroborating the concept that the 5′TOP motif is not a translational element per se; more appropriately, it coordinates a posttranscriptional mechanism that has an impact at the translational level being the 40*S* subunit an essential element of the 5′TOP stability complex.

The capacity of cells to reestablish the anabolism at the translational level potentially avoids unnecessary gene regulatory mechanism that a resting cell cannot energetically afford in terms of RNA transcription, maturation, nuclear export, and translational engagement. Such a critical paradigm is provided by the metabolic awakening of oocytes after fecundation, in which the zygote relies on the translational engagement of maternal storages of RP mRNAs that rapidly populate the polyribosomes to reconstitute the ribosome biogenesis rate necessary since the first step of the developmental program (*20*). Consistent with this observation, LARP1 depletion produced an oogenesis defect either in *C. Elegans* or in *Drosophila melanogaster* (*45*, *46*). With respect to cancer, the rapid growth of solid tumors frequently generates local nutrient and oxygen shortages due to the high demand outstripping the vascular supply, which, in turn, can generate a metabolic adaptation of resistant clones. The mechanism we describe in this study highlights a unique aspect of cellular plasticity, which may confer a selective advantage for resistant tumor cells to promptly regrow when neovascularization occurs and external conditions become more permissive. As many chemotherapeutics regimens also restrain mTOR activity and cellular metabolism, it is likely that the 40*S*-LARP1 complex could prepare the cells in quickly reestablishing the protein synthetic capacity after treatment is halted, a prerequisite to regrow and proliferate. In this regard, it has been shown that LARP1 expression correlates with the malignancy status in ovarian cancer and hepatocellular carcinoma (*47*, *48*) as well as bad prognosis marker in colorectal cancer (*49*), supporting a potential role of the mTOR/40*S*-LARP1 axis in the tumorigenesis and in tumor recurrence after treatments.

Functional aspects of LARP1 mechanism of action

LARP1 was identified as part of the phospho-proteome controlled by acute mTOR inhibition (*25*, *26*). The following studies have shown that mTOR is able to phosphorylate in vitro LARP1 at specific residues (*27*) and that mTOR inhibition increases the affinity of LARP1 for 5′TOP mRNAs (*24*). Consistent with these findings, we observed an increase in 40*S*-LARP1-5′TOP complex formation after mTOR inhibition, suggesting that the hypophosphorylated form of LARP1 has a stronger affinity for 5′TOP mRNAs, as also verified in Jia *et al.* (*28*). A major effort in identifying the LARP1 phospho-residues controlling the binding of LARP1 and 5′TOP mRNAs is needed to better understand the interplay between mTOR signaling and LARP1-5′TOP interaction. The observation that the serines at the positions 689 and 697 of LARP1, located just outside the DM15 5′TOP-binding domain, are direct substrates of mTOR suggests, if confirmed in vivo, that these phosphorylations can sterically modify the DM15 domain of LARP1 to change the affinity for 5′TOP mRNAs as also hypothesized by others (*50*). The hypothesis that mTOR inhibition controls the formation of 40*S*-LARP1-5′TOP complex is supported by the experiments carried out in *Tsc2*$^{-/-}$ MEFs where mTOR signaling is maintained active upon either serum or amino acid deprivation (Fig. 4, E to H), partly recapitulating the effects observed in LARP1 KO cells following the same treatments (Fig. 4, A to D). Although we cannot exclude that mTORC2 might play a role depending on the stimulus, the inhibition of mTOR complex 1 appeared to be critical in controlling the 5′TOP stabilization and the 40*S*-LARP1 redistribution (figs. S1G

and S4G, and Fig. 4, E to H). Consistent with this, previous studies have shown that 4EBP1 and 4EBP2 are necessary to mediate the translational inhibition of 5′TOP mRNAs upon acute mTOR inhibition (*33*, *34*). Active-site mTOR inhibitor treatment in 4EBP1/2 KO MEFs phenocopies the effects observed in LARP1 KO cells with an impaired accumulation of 5′TOP mRNAs with the nonpolysomes (*34*), suggesting that 4EBPs and LARP1 in their hypophosphorylated forms are both necessary to preserve the 5′TOP mRNAs. A similar reasoning is valid for the two RNA binding protein TIA1 (TIA1 cytotoxic granule associated RNA binding protein) and TIAR (TIA1 related) that were demonstrated to be necessary in response to amino acid deprivation for blunting 5′TOP mRNA translation (*31*), but not for pharmacological mTOR inhibition (*34*). Also, in this context, LARP1 KO cells phenocopy the effects of TIA1/TIAR depletion after amino acid deprivation (Fig. 4, A and B). A reasonable scenario is the 40*S*-LARP1 complex being the hub for binding of other cofactors to interact with 5′TOP mRNAs in response to specific mTOR-inhibiting stimuli. Mechanistically, one possible interpretation is that the polysomal-anchored LARP1, when receiving an inhibitory signal by mTOR, could hamper the translational reinitiation determining a runoff of actively translating ribosomes, which is compatible with the short time required for the 40*S*-LARP1-5′TOP accumulation with the nonpolysomes, all together protecting the protein synthetic capacity of the cell in the form of mRNAs.

METHODS

Cell culture

HCT116 human colorectal carcinoma cell lines and A549 cells were obtained from the American Type Culture Collection and maintained in Dulbecco's modified Eagle's medium (DMEM) supplemented with 10% heat-inactivated fetal bovine serum (Sigma-Aldrich, St Louis, MO, USA). RT4 bladder carcinoma cell line was provided by A. Rovira. Double stable inducible HCT116 rtTA (reverse tetracycline-controlled transactivator)/TetO (tetracycline operator)-WT-L32TOP–β-globin–MS2(12X) or HCT116 rtTA/TetO-MU-L32TOP–β-globin-MS2(12X) were previously described (*22*). Tsc2$^{+/+}$; Trp53$^{-/-}$ and Tsc2$^{-/-}$; Trp53$^{-/-}$ MEFs (*51*) were provided by A. Efeyan; and Atg7$^{+/+}$ and Atg7$^{-/-}$ MEFs (*52*) were provided by M. Komatsu. All MEFs were maintained in DMEM supplemented with 10% heat-inactivated fetal bovine serum.

Generation of LARP1 KO cells by CRISPR-Cas9

HCT116 cells were transfected with pX458 plasmid (Addgene catalog number 48138) containing CRISPR-Cas9–targeting exon 5 of the LARP1 gene using Lipofectamine 2000 transfection reagent (Invitrogen). As the pX458 plasmid contains green fluorescent protein, single-cell sorting was performed 48 hours after transfection using BD FACSAria (BD Biosciences), and individual clones were cultivated and subsequently analyzed for LARP1 expression by immunoblotting, leading to the isolation of the LARP1 KO clone 68 (KO #68) and clone 72 (KO #72). The same procedure was carried out to generate A549 LARP1 KO cells. Primers targeting the exon 5 of LARP1 are reported in table S1.

Reagents and plasmids

RNAimax transfection reagent, TRIzol RNA extraction reagent, Click-iT protein reaction buffer kit, Click-iT AHA (L-azidohomoalanine), and the biotin-alkyne conjugate were purchased from Invitrogen (Carlsbad, CA, USA). The Pierce NeutrAvidin Agarose beads were purchased from Thermo Fisher Scientific. TAK228 (formerly MLN0128 and INK-128) was from Selleck chemicals. EN3HANCE autoradiography enhancer, ^{3}H-uridine, and ^{3}H–L-leucine were purchased from PerkinElmer. The SYBR Green qPCR Kit was from Roche (Basel, Switzerland). qPCR PrimeTime master mix and FAM-Cy5–labeled probes were from IDT (Integrated DNA Technologies). The Bradford reagent was from Bio-Rad. The polyclonal anti-LARP1 to detect the mammalian LARP1 protein and anti-L5 antibodies was from Bethyl Laboratories. Anti-LARP1 for MEF-derived samples was from Proteintech as well as the anti-NUFIP1 (12515-1-AP). The anti-S23 (clone SJ-K2) and anti-S6 (clone C-8) monoclonal antibodies were purchased from Santa Cruz Biotechnology, the LC3 polyclonal antibody was purchased from MBL, and the anti–β-actin (clone AC-74) and anti–α-tubulin (clone B-5-1-2) monoclonal antibodies were purchased from Sigma-Aldrich. The anti–phospho S6K1 (T389), anti–phospho 4EBP1 (S65), anti–phospho S6 (S235/236), anti–phospho EIF2α (S51), anti–phospho AKT (S473), anti-4EBP1, anti-TSC2 (clone D39F12), and anti-GAPDH (clone 14C10) were purchased from Cell Signaling Technology. Anti-PABP [poly(A) binding protein] was from Abcam. MagnaCHIP Protein A/G magnetic bead mix was from Millipore. Goat anti–[mouse immunoglobulin G (IgG)]–peroxidase conjugate and goat anti–(rabbit IgG)–peroxidase conjugate were from Dako. The placental ribonuclease (RNase) inhibitor was purchased from NEB (New England Biolabs). The sequences of small interfering RNAs (siRNAs) used in the experiments—siNS, siRPS6, and siRPL7a—are reported in table S1.

Protein analysis

Cell protein extracts for Western blot analysis were prepared by using a 1% SDS lysis buffer [50 mM tris (pH 7.4) and 1% SDS] supplemented with the protease inhibitor cocktail (Sigma-Aldrich), phosphatase inhibitor cocktail 2 (Sigma-Aldrich), 2 mM sodium orthovanadate, and benzonase (100 U/ml). After lysis, cell lysates were incubated 30′ on ice followed by centrifugation at 13,000 rpm for 10′. Protein concentrations were determined for supernatants by the BCA assay (Pierce). Twenty-five micrograms of total protein extracts was resuspended in Laemmli SDS sample buffer (1×) and boiled at 95°C for 10 min. Proteins were separated on 10% SDS–polyacrylamide gels by electrophoresis and transferred to polyvinylidene difluoride (PVDF) membranes (GE Healthcare Life Science). Blots were stained with amido black to confirm equal loading and transfer of proteins and then reacted with the Western blots probed with the indicated antibodies.

LARP1 distribution on sucrose gradients was analyzed by dot blot. Twenty percent volume of each fraction supplemented with Laemmli SDS sample buffer and boiled for 10 min at 95°C were loaded on the dot blot apparatus and transferred on PVDF. The membrane was stained with amido black and incubated with the anti-LARP1 antibody. Immunoblots were developed using secondary horseradish peroxidase–coupled antibodies and an enhanced chemiluminescence kit (GE Healthcare) (*22*).

Real-time PCR

Total cellular RNAs were isolated using TRIzol reagent (Invitrogen) according to the manufacturer's instructions. Complementary DNA synthesis and quantitative real-time PCR were performed as described previously as concerned with the SYBR green detection (*53*)

or with RNA-specific hydrolysis probes at 125 nM final concentration, in combination with the same primer pairs used for SYBR green qPCRs at 500 nM and the PrimeTime master mix (IDT). For the luciferase normalization, cells were harvested in an equal volume of cold phosphate-buffered saline (PBS), and 1/10 of the cell suspension was assayed for genomic DNA (gDNA) concentration, which we verified reflecting the cell number in the culturing conditions tested. The remaining volume of cells was centrifuged, and cell pellet was resuspended in TRIzol and spiked with an amount of Firefly Luciferase mRNA (Promega, L456A), proportional to the gDNA content, according to the ratio, 0.025 ng of Firefly mRNA per microgram of gDNA. The samples were processed as described above, and the levels of RPs, non-TOP mRNAs, or rRNA were normalized to luciferase mRNA. The sequences of primers used to amplify RPL5, RPL11, RPL7a, RPS6, GAPDH, 18*S* rRNA, β-actin, and Firefly are reported in table S1.

Autoradiographic analysis of rRNA synthesis

To label newly synthesized RNA, cells were incubated for 2 hours with [^{3}H]-uridine (1.2 μCi/ml; PerkinElmer). Cells were counted, and the total RNA corresponding to an equal number of cells for each condition was separated by Northern blot having for the time = 0 1 μg of total RNA. Agarose-resolved RNAs were transferred to Hybond N+ membrane (GE Healthcare). After ultraviolet cross-linking, the membrane was sprayed with EN3HANCE (PerkinElmer) and exposed to Kodak BioMax MS film (Kodak) at −80°C for 1 week (*22*). Nascent rRNA was detected by autoradiography.

Polysome profile analysis

Distribution of mRNAs across sucrose gradients was performed as described earlier (*54*), except for minor modifications. Briefly, 10^6 HCT116 cells were plated in 100-mm dish and transfected with the indicated treatment. Cycloheximide (CHX) was added to the medium at 37°C for 5 min at a concentration of 100 μg/ml. Cells were washed twice with cold PBS supplemented with CHX, scraped on ice, and pelleted by centrifugation at 3000 rpm for 3′ in cold. Cell pellets were resuspended in 250 μl of hypotonic lysis buffer [1.5 mM KCl, 2.5 mM $MgCl_2$, 5 mM tris HCl (pH 7.4), 1 mM dithiothreitol (DTT), 1% sodium deoxycholate, 1% Triton X-100, and CHX (100 μg/ml)] supplemented with mammalian protease inhibitors (Sigma-Aldrich) and RNase inhibitor (NEB) at a concentration of 100 U/ml and left in ice for 5′. Cell lysates were cleared of debris and nuclei by centrifugation for 5′ at 13,000 rpm. Protein concentrations were determined by BCA assay, and equal amount of polysomal lysate (500 to 1000 μg, depending on the experiment) was loaded on 10 to 50% sucrose linear gradients generated with a BIOCOMP gradient master and containing 80 mM NaCl, 5 mM $MgCl_2$, 20 mM tris HCl (pH 7.4), 1 mM DTT, and RNase inhibitor (10 U/ml). Gradients were centrifuged on a SW40 rotor for 3 hours and 30 min at 35,000 rpm or 2 hours and 55 min at 35,000 rpm as indicated in the figure legends. Gradients were analyzed on a BIOCOMP gradient station and collected in 12 or 13 fractions ranging from light to heavy sucrose. Fractions were supplemented with SDS at a final concentration of 1% and placed for 10 min at 65°C. To each fraction was added 1 ng of firefly luciferase mRNA, followed by phenol-chloroform extraction and precipitation with isopropanol. Purified RNAs from each fraction were reverse-transcribed and subjected to qPCR. mRNA quantification was normalized to firefly mRNA. All sucrose gradient fractionations have been repeated at least twice in independent experiments. The profiles and RT-qPCR analyses shown in the figures are representative experiments (*22*).

Sample preparation for RNA-seq

After the indicated treatment, polysomal lysates from parental or LARP1 KO control HCT116 cells were resolved by 10 to 50% sucrose gradient fractionation as described above. For each sample, 20% volume of nonpolysomal fractions from 40*S* to 80*S* peaks (gray area) were pooled and spiked with a library of RNAs for normalization purposes across samples [ERCC (External RNA Controls Consortium) spike-in mix, Thermo Fisher Scientific]. One microgram of RNAs from two biological replicates from parental and LARP1 KO pools was depleted of rRNA with the Ribozero human, mouse, and rat kit (Illumina), and libraries for RNA-seq were prepared. To identify the TSS of mRNAs protected by LARP1 with nonpolysomes, 1 μg of two parental RNAs was treated with alkalyne phosphates to blunt spourious 5′ termini, and calf intestinal phosphatase–treated RNAs were decapped with tobacco alkaline phoshpatase (TAP; EpiCentre Technologies). Exposed 5′ termini were ligated to an RNA oligo (table S1), and then library was processed as above for RNA-seq analysis.

RNA-seq analysis

All libraries were sequenced on Illumina Novaseq 6000 platform in pair-end mode, resulting in 150-base length reads at Macrogen, Korea (GSE186779 deposited at Gene Expression Omnibus). Library depths were oscillated between 24 to 37 million mappable paired-end reads. RNA-seq reads were trimmed with bbduk from BBTools suite (*55*) to remove low-quality bases, adapters, and recombinant DNA. FastQC (*56*) was used for quality control of the reads. Trimmed reads were aligned against human reference transcriptome GRCh38 with STAR v(2.6) (*57*). Transcript and gene abundance quantification was performed with RSEM v(1.3.0) (*58*). GENCODE v29 was used for gene and transcript annotation. For differential expression analysis, we used the statistical methods implemented in the DESeq2 R package (*59*). ERCC spike-ins were used to calculate normalization factors. Significance threshold was set at log 2 fold change of ≥ 1 and $-\log_{10} Q$ value of ≥ 2 (Fig. 5C).

TSS analysis

For the TSS analysis, we selected the sequencing reads that included part of the 3′ region of the RNA adapter oligo sequence ligated to the TAP-exposed 5′ termini (i.e., reads with at least the following 15 bp: "CTGGCTTTGATGAAA") using GNU grep. We choose this specific oligo sequence to maximize both the oligo length and the number of reads with it. Next, we trimmed the oligo sequence with bbduk from BBTools suite (*55*) and aligned the sequencing reads to the human reference genome GRCh38 with STAR v(2.6) (*57*). We concatenated the two replicates with Samtools cat (*60*) to increase the depth of coverage, obtaining a single alignment file with 282,495 mappable paired-end reads. We split the alignment file to obtain one per transcript, considering only protein coding, long noncoding, and antisense transcripts based on GENCODE v19 annotation reference. We computed the coverage for the reference nucleotide systematically for all transcripts using Samtools mpileup (*60*). TSS isoforms were determined at genome positions with an increase of coverage of more than 5% of the total coverage of a given transcript. We used GNU awk for performing calculations. We annotated as TOP isoforms those with the 5′ motif sequence "C[C/T][C/T]" and computed the percentage of TOP isoforms per gene using R. We made a bedgraph file with TSS coverage of all genes to visualize on IGV. In Fig. 5E, the corresponding circle-starting red lines display the 5′TOP-isoform transcripts.

De novo protein analysis

For Click-iT de novo synthesis analysis, cells were treated as indicated in Fig. 6C. Before lysis, cells were placed in methionine-free DMEM supplemented with 25 μM AHA for 2 hours. AHA-labeled proteins were chemically processed according to manufacturer's protocol, and 200 μg of biotin-alkyne–conjugated proteins were resuspended in 500 μl of PBS, 150 mM NaCl, 0.1% SDS, and protease inhibitors and incubated 2 hours at room temperature with NeutrAvidin Agarose beads. NeutrAvidin biotin conjugates were washed three times with 500 μl of wash solution [50 mM tris-HCl (pH 7.4), 150 mM NaCl, and 0.1% SDS], resuspended in 2× Laemmli buffer, resolved on 4 to 15% bis-tris polyacrylamide gel, blotted on PVDF, and probed with the indicated antibodies (*22*). For Global Click-iT analysis (table S3), a replicate of the culturing/labeling protocol described in Fig. 6C (excluding the growing condition) was performed. Duplicate samples deriving from 2E6 cells per condition were processed according to the manufacturer protocol (Click-iT Protein Enrichment kit, ThermoFisher) and analyzed by liquid chromatography–mass spectrometry. AHA-labeled proteins with a linear fold change of 1.8 between TAK 48 hours + washout/TAK 48 hours where identified as translationally up-regulated (table S3).

For global protein synthesis rate, cells were cultured in triplicates as described in Fig. 6E and pulsed in the last 30′ with 10 μCi of ^{3}H-leucine in triplicates. Cells were washed twice with cold PBS and lysed with radioimmunoprecipitation assay buffer, and whole-cell lysate supernatant was cleared by centrifugation. To get rid of unincorporated ^{3}H-leucine, trichloroacetic acid precipitation was carried out as described previously (*30*), and protein pellets were resuspended with 1% SDS at 50°C. An aliquot of ^{3}H-leucine–incorporated protein lysates was used for BCA quantification, while the rest was analyzed at the scintillation counter. The ratios of counts per minutes over microgram of protein were calculated (*22*).

Cell cycle analysis

Cell cycle analysis was performed using the propidium iodide cell cycle reagent protocol as described previously (*61*). Briefly, HCT116 cells were grown overnight in DMEM supplemented with 10% serum and then treated with 250 nM TAK228 or with normal growing medium. After 48 hours, cells were harvested, fixed with 70% ethanol, and treated for 30 min with propidium iodide solution at 37°C. Actinomycin D treatment at 5 nM was used as control of cell death. Samples were analyzed using the FACSCanto System. The data are representative of three different experiments.

Statistical analysis

Statistical analysis was performed using GraphPad Prism V8.0. Data are presented as means ± SEM. Comparisons were performed with a two-way analysis of variance (ANOVA) multiple comparisons test as specified in the figure legends.

SUPPLEMENTARY MATERIALS

Supplementary material for this article is available at https://science.org/doi/10.1126/sciadv.abg9275

View/request a protocol for this paper from *Bio-protocol*.

REFERENCES AND NOTES

1. S. Volarevic, M. J. Stewart, B. Ledermann, F. Zilberman, L. Terracciano, E. Montini, M. Grompe, S. C. Kozma, G. Thomas, Proliferation, but not growth, blocked by conditional deletion of 40S ribosomal protein S6. *Science* **288**, 2045–2047 (2000).
2. R. A. Saxton, D. M. Sabatini, mTOR signaling in growth, metabolism, and disease. *Cell* **168**, 960–976 (2017).
3. M. Laplante, D. M. Sabatini, mTOR signaling in growth control and disease. *Cell* **149**, 274–293 (2012).
4. R. A. J. Signer, J. A. Magee, A. Salic, S. J. Morrison, Haematopoietic stem cells require a highly regulated protein synthesis rate. *Nature* **509**, 49–54 (2014).
5. G. A. Wyant, M. Abu-Remaileh, E. M. Frenkel, N. N. Laqtom, V. Dharamdasani, C. A. Lewis, S. H. Chan, I. Heinze, A. Ori, D. M. Sabatini, NUFIP1 is a ribosome receptor for starvation-induced ribophagy. *Science* **360**, 751–758 (2018).
6. F. Amaldi, I. Bozzoni, E. Beccari, P. Pierandrei-Amaldi, Expression of ribosomal protein genes and regulation of ribosome biosynthesis in Xenopus development. *Trends Biochem. Sci.* **14**, 175–178 (1989).
7. A. Gentilella, S. C. Kozma, G. Thomas, A liaison between mTOR signaling, ribosome biogenesis and cancer. *Biochim. Biophys. Acta* **1849**, 812–820 (2015).
8. C. U. Hellen, P. Sarnow, Internal ribosome entry sites in eukaryotic mRNA molecules. *Genes Dev.* **15**, 1593–1612 (2001).
9. J. Zhou, J. Wan, X. Gao, X. Zhang, S. R. Jaffrey, S. B. Qian, Dynamic m^{6}A mRNA methylation directs translational control of heat shock response. *Nature* **526**, 591–594 (2015).
10. R. A. Coots, X.-M. Liu, Y. Mao, L. Dong, J. Zhou, J. Wan, X. Zhang, S.-B. Qian, m^{6}A facilitates eIF4F-independent mRNA translation. *Mol. Cell* **68**, 504–514.e7 (2017).
11. Z. Shi, K. Fujii, K. M. Kovary, N. R. Genuth, H. L. Rost, M. N. Teruel, M. Barna, Heterogeneous ribosomes preferentially translate distinct subpools of mRNAs genome-wide. *Mol. Cell* **67**, 71–83.e7 (2017).
12. D. Simsek, G. C. Tiu, R. A. Flynn, G. W. Byeon, K. Leppek, A. F. Xu, H. Y. Chang, M. Barna, The mammalian ribo-interactome reveals ribosome functional diversity and heterogeneity. *Cell* **169**, 1051–1065.e18 (2017).
13. M. M. Parks, C. M. Kurylo, R. A. Dass, L. Bojmar, D. Lyden, C. T. Vincent, S. C. Blanchard, Variant ribosomal RNA alleles are conserved and exhibit tissue-specific expression. *Sci. Adv.* **4**, eaao0665 (2018).
14. A. Sriram, J. Bohlen, A. A. Teleman, Translation acrobatics: How cancer cells exploit alternate modes of translational initiation. *EMBO Rep.* **19**, (2018).
15. R. A. J. Signer, L. Qi, Z. Zhao, D. Thompson, A. A. Sigova, Z. P. Fan, G. N. DeMartino, R. A. Young, N. Sonenberg, S. J. Morrison, The rate of protein synthesis in hematopoietic stem cells is limited partly by 4E-BPs. *Genes Dev.* **30**, 1698–1703 (2016).
16. L. Da Costa, G. Narla, T. N. Willig, L. L. Peters, M. Parra, J. Fixler, G. Tchernia, N. Mohandas, Ribosomal protein S19 expression during erythroid differentiation. *Blood* **101**, 318–324 (2003).
17. J. Flygare, S. Karlsson, Diamond-Blackfan anemia: Erythropoiesis lost in translation. *Blood* **109**, 3152–3154 (2007).
18. E. Llorens-Bobadilla, S. Zhao, A. Baser, G. Saiz-Castro, K. Zwadlo, A. Martin-Villalba, Single-cell transcriptomics reveals a population of dormant neural stem cells that become activated upon brain injury. *Cell Stem Cell* **17**, 329–340 (2015).
19. S. Blanco, R. Bandiera, M. Popis, S. Hussain, P. Lombard, J. Aleksic, A. Sajini, H. Tanna, R. Cortes-Garrido, N. Gkatza, S. Dietmann, M. Frye, Stem cell function and stress response are controlled by protein synthesis. *Nature* **534**, 335–340 (2016).
20. P. Pierandrei-Amaldi, E. Beccari, I. Bozzoni, F. Amaldi, Ribosomal protein production in normal and anucleolate Xenopus embryos: Regulation at the posttranscriptional and translational levels. *Cell* **42**, 317–323 (1985).
21. E. Zanin, A. Pacquelet, C. Scheckel, R. Ciosk, M. Gotta, LARP-1 promotes oogenesis by repressing *fem-3* in the *C. elegans* germline. *J. Cell Sci.* **123**, 2717–2724 (2010).
22. A. Gentilella, F. D. Morón-Duran, P. Fuentes, G. Zweig-Rocha, F. Riaño-Canalias, J. Pelletier, M. Ruiz, G. Turón, J. Castaño, A. Tauler, C. Bueno, P. Menéndez, S. C. Kozma, G. Thomas, Autogenous control of 5′TOP mRNA stability by 40S ribosomes. *Mol. Cell* **67**, 55–70.e4 (2017).
23. J. Tcherkezian, M. Cargnello, Y. Romeo, E. L. Huttlin, G. Lavoie, S. P. Gygi, P. P. Roux, Proteomic analysis of cap-dependent translation identifies LARP1 as a key regulator of 5′TOP mRNA translation. *Genes Dev.* **28**, 357–371 (2014).
24. B. D. Fonseca, C. Zakaria, J. J. Jia, T. E. Graber, Y. Svitkin, S. Tahmasebi, D. Healy, H. D. Hoang, J. M. Jensen, I. T. Diao, A. Lussier, C. Dajadian, N. Padmanabhan, W. Wang, E. Matta-Camacho, J. Hearnden, E. M. Smith, Y. Tsukumo, A. Yanagiya, M. Morita, E. Petroulakis, J. L. Gonzalez, G. Hernandez, T. Alain, C. K. Damgaard, La-related protein 1 (LARP1) represses terminal oligopyrimidine (TOP) mRNA translation downstream of mTOR complex 1 (mTORC1). *J. Biol. Chem.* **290**, 15996–16020 (2015).
25. P. P. Hsu, S. A. Kang, J. Rameseder, Y. Zhang, K. A. Ottina, D. Lim, T. R. Peterson, Y. Choi, N. S. Gray, M. B. Yaffe, J. A. Marto, D. M. Sabatini, The mTOR-regulated phosphoproteome reveals a mechanism of mTORC1-mediated inhibition of growth factor signaling. *Science* **332**, 1317–1322 (2011).
26. Y. Yu, S. O. Yoon, G. Poulogiannis, Q. Yang, X. M. Ma, J. Villen, N. Kubica, G. R. Hoffman, L. C. Cantley, S. P. Gygi, J. Blenis, Phosphoproteomic analysis identifies Grb10 as an mTORC1 substrate that negatively regulates insulin signaling. *Science* **332**, 1322–1326 (2011).

27. S. Hong, M. A. Freeberg, T. Han, A. Kamath, Y. Yao, T. Fukuda, T. Suzuki, J. K. Kim, K. Inoki, LARP1 functions as a molecular switch for mTORC1-mediated translation of an essential class of mRNAs. *eLife* **6**, e25237 (2017).
28. J. J. Jia, R. M. Lahr, M. T. Solgaard, B. J. Moraes, R. Pointet, A. D. Yang, G. Celucci, T. E. Graber, H. D. Hoang, M. R. Niklaus, I. A. Pena, A. K. Hollensen, E. M. Smith, M. Chaker-Margot, L. Anton, C. Dajadian, M. Livingstone, J. Hearnden, X. D. Wang, Y. Yu, T. Maier, C. K. Damgaard, A. J. Berman, T. Alain, B. D. Fonseca, mTORC1 promotes TOP mRNA translation through site-specific phosphorylation of LARP1. *Nucleic Acids Res.* **49**, 3461–3489 (2021).
29. A. Hernandez-Prat, A. Rodriguez-Vida, N. Juanpere-Rodero, O. Arpi, S. Menendez, L. Soria-Jimenez, A. Martinez, N. Iarchouk, F. Rojo, J. Albanell, R. Brake, A. Rovira, J. Bellmunt, Novel oral mTORC1/2 inhibitor TAK-228 has synergistic antitumor effects when combined with paclitaxel or PI3Kα inhibitor TAK-117 in preclinical bladder cancer models. *Mol. Cancer Res.* **17**, 1931–1944 (2019).
30. S. Fumagalli, A. Di Cara, A. Neb-Gulati, F. Natt, S. Schwemberger, J. Hall, G. F. Babcock, R. Bernardi, P. P. Pandolfi, G. Thomas, Absence of nucleolar disruption after impairment of 40S ribosome biogenesis reveals an rpL11-translation-dependent mechanism of p53 induction. *Nat. Cell Biol.* **11**, 501–508 (2009).
31. C. K. Damgaard, J. Lykke-Andersen, Translational coregulation of 5'TOP mRNAs by TIA-1 and TIAR. *Genes Dev.* **25**, 2057–2068 (2011).
32. C. Demetriades, M. Plescher, A. A. Teleman, Lysosomal recruitment of TSC2 is a universal response to cellular stress. *Nat. Commun.* **7**, 10662 (2016).
33. A. C. Hsieh, Y. Liu, M. P. Edlind, N. T. Ingolia, M. R. Janes, A. Sher, E. Y. Shi, C. R. Stumpf, C. Christensen, M. J. Bonham, S. Wang, P. Ren, M. Martin, K. Jessen, M. E. Feldman, J. S. Weissman, K. M. Shokat, C. Rommel, D. Ruggero, The translational landscape of mTOR signalling steers cancer initiation and metastasis. *Nature* **485**, 55–61 (2012).
34. C. C. Thoreen, L. Chantranupong, H. R. Keys, T. Wang, N. S. Gray, D. M. Sabatini, A unifying model for mTORC1-mediated regulation of mRNA translation. *Nature* **485**, 109–113 (2012).
35. I. Ben-Sahra, J. J. Howell, J. M. Asara, B. D. Manning, Stimulation of de novo pyrimidine synthesis by growth signaling through mTOR and S6K1. *Science* **339**, 1323–1328 (2013).
36. I. Ben-Sahra, G. Hoxhaj, S. J. H. Ricoult, J. M. Asara, B. D. Manning, mTORC1 induces purine synthesis through control of the mitochondrial tetrahydrofolate cycle. *Science* **351**, 728–733 (2016).
37. Y. Zhang, J. Nicholatos, J. R. Dreier, S. J. H. Ricoult, S. B. Widenmaier, G. S. Hotamisligil, D. J. Kwiatkowski, B. D. Manning, Coordinated regulation of protein synthesis and degradation by mTORC1. *Nature* **513**, 440–443 (2014).
38. T. R. Peterson, S. S. Sengupta, T. E. Harris, A. E. Carmack, S. A. Kang, E. Balderas, D. A. Guertin, K. L. Madden, A. E. Carpenter, B. N. Finck, D. M. Sabatini, mTOR complex 1 regulates lipin 1 localization to control the SREBP pathway. *Cell* **146**, 408–420 (2011).
39. I. Ben-Sahra, B. D. Manning, mTORC1 signaling and the metabolic control of cell growth. *Curr. Opin. Cell Biol.* **45**, 72–82 (2017).
40. M. Morita, S. P. Gravel, V. Chenard, K. Sikstrom, L. Zheng, T. Alain, V. Gandin, D. Avizonis, M. Arguello, C. Zakaria, S. McLaughlan, Y. Nouet, A. Pause, M. Pollak, E. Gottlieb, O. Larsson, J. St-Pierre, I. Topisirovic, N. Sonenberg, mTORC1 controls mitochondrial activity and biogenesis through 4E-BP-dependent translational regulation. *Cell Metab.* **18**, 698–711 (2013).
41. R. J. O. Dowling, I. Topisirovic, T. Alain, M. Bidinosti, B. D. Fonseca, E. Petroulakis, X. Wang, O. Larsson, A. Selvaraj, Y. Liu, S. C. Kozma, G. Thomas, N. Sonenberg, mTORC1-mediated cell proliferation, but not cell growth, controlled by the 4E-BPs. *Science* **328**, 1172–1176 (2010).
42. J. H. Wilbertz, F. Voigt, I. Horvathova, G. Roth, Y. Zhan, J. A. Chao, Single-molecule imaging of mRNA localization and regulation during the integrated stress response. *Mol. Cell* **73**, 946–958.e7 (2019).
43. L. Philippe, A. M. G. van den Elzen, M. J. Watson, C. C. Thoreen, Global analysis of LARP1 translation targets reveals tunable and dynamic features of 5' TOP motifs. *Proc. Natl. Acad. Sci. U.S.A.* **117**, 5319–5328 (2020).
44. A.-A. Zimta, A. B. Tigu, C. Braicu, C. Stefan, C. Ionescu, I. Berindan-Neagoe, An emerging class of long non-coding RNA with oncogenic role arises from the snoRNA host genes. *Front. Oncol.* **10**, 389 (2020).
45. K. Nykamp, M.-H. Lee, J. Kimble, *C. elegans* La-related protein, LARP-1, localizes to germline P bodies and attenuates Ras-MAPK signaling during oogenesis. *RNA* **14**, 1378–1389 (2008).
46. Y. Zhang, Z.-H. Wang, Y. Liu, Y. Chen, N. Sun, M. Gucek, F. Zhang, H. Xu, PINK1 inhibits local protein synthesis to limit transmission of deleterious mitochondrial DNA mutations. *Mol. Cell* **73**, 1127–1137.e5 (2019).
47. C. Xie, L. Huang, S. Xie, D. Xie, G. Zhang, P. Wang, L. Peng, Z. Gao, LARP1 predict the prognosis for early-stage and AFP-normal hepatocellular carcinoma. *J. Transl. Med.* **11**, 272 (2013).
48. T. G. Hopkins, M. Mura, H. A. Al-Ashtal, R. M. Lahr, N. Abd-Latip, K. Sweeney, H. Lu, J. Weir, M. El-Bahrawy, J. H. Steel, S. Ghaem-Maghami, E. O. Aboagye, A. J. Berman, S. P. Blagden, The RNA-binding protein LARP1 is a post-transcriptional regulator of survival and tumorigenesis in ovarian cancer. *Nucleic Acids Res.* **44**, 1227–1246 (2016).
49. L. Ye, S. T. Lin, Y. S. Mi, Y. Liu, Y. Ma, H. M. Sun, Z. H. Peng, J. W. Fan, Overexpression of LARP1 predicts poor prognosis of colorectal cancer and is expected to be a potential therapeutic target. *Tumour Biol.* **37**, 14585–14594 (2016).
50. R. M. Lahr, B. D. Fonseca, G. E. Ciotti, H. A. Al-Ashtal, J. J. Jia, M. R. Niklaus, S. P. Blagden, T. Alain, A. J. Berman, La-related protein 1 (LARP1) binds the mRNA cap, blocking eIF4F assembly on TOP mRNAs. *eLife* **6**, e24146 (2017).
51. H. Zhang, G. Cicchetti, H. Onda, H. B. Koon, K. Asrican, N. Bajraszewski, F. Vazquez, C. L. Carpenter, D. J. Kwiatkowski, Loss of Tsc1/Tsc2 activates mTOR and disrupts PI3K-Akt signaling through downregulation of PDGFR. *J. Clin. Invest.* **112**, 1223–1233 (2003).
52. M. Komatsu, S. Waguri, T. Ueno, J. Iwata, S. Murata, I. Tanida, J. Ezaki, N. Mizushima, Y. Ohsumi, Y. Uchiyama, E. Kominami, K. Tanaka, T. Chiba, Impairment of starvation-induced and constitutive autophagy in Atg7-deficient mice. *J. Cell Biol.* **169**, 425–434 (2005).
53. A. Gentilella, K. Khalili, BAG3 expression in glioblastoma cells promotes accumulation of ubiquitinated clients in an Hsp70-dependent manner. *J. Biol. Chem.* **286**, 9205–9215 (2011).
54. S. Fumagalli, V. V. Ivanenkov, T. Teng, G. Thomas, Suprainduction of p53 by disruption of 40S and 60S ribosome biogenesis leads to the activation of a novel G2/M checkpoint. *Genes Dev.* **26**, 1028–1040 (2012).
55. B. Bushnell, BBtools. BBMap short read aligner, and other bioinformatic tools. Available online at: https://sourceforge.net/projects/bbmap.
56. S. Andrews, FastQC: a quality control tool for high throughput sequence data. (2010); Available online at: https://www.bioinformatics.babraham.ac.uk/projects/fastqc/.
57. A. Dobin, C. A. Davis, F. Schlesinger, J. Drenkow, C. Zaleski, S. Jha, P. Batut, M. Chaisson, T. R. Gingeras, STAR: Ultrafast universal RNA-seq aligner. *Bioinformatics* **29**, 15–21 (2013).
58. B. Li, C. N. Dewey, RSEM: Accurate transcript quantification from RNA-Seq data with or without a reference genome. *BMC Bioinformatics* **12**, 323 (2011).
59. M. I. Love, W. Huber, S. Anders, Moderated estimation of fold change and dispersion for RNA-seq data with DESeq2. *Genome Biol.* **15**, 550 (2014).
60. H. Li, B. Handsaker, A. Wysoker, T. Fennell, J. Ruan, N. Homer, G. Marth, G. Abecasis, R. Durbin; 1000 Genome Project Data Processing Subgroup, The sequence alignment/map format and SAMtools. *Bioinformatics* **25**, 2078–2079 (2009).
61. A. Gentilella, G. Passiatore, S. Deshmane, M. C. Turco, K. Khalili, Activation of BAG3 by Egr-1 in response to FGF-2 in neuroblastoma cells. *Oncogene* **27**, 5011–5018 (2008).

Acknowledgments: We thank past and present members of the Laboratory of Cancer Metabolism and all people at IDIBELL who supported the development of this study. We feel an immense gratitude to G. Thomas for critical comments and precious suggestions throughout the whole study, S. Kozma for the generous support and for sharing reagents, and to A. Efeyan who provided *Tsc2*$^{-/-}$*; p53*$^{-/-}$ MEF and for the insightful discussions. **Funding:** This study has been funded by Ministerio de Ciencia, Innovación y Universidades, which is part of Agencia Estatal de Investigación (AEI), through the Plan Nacional "Excelencia" grant number SAF2017-84301-P (cofunded by European Regional Development Fund. ERDF, a way to build Europe), by the "Asociación Española Contra el Cancer" (AECC; LABAE20040GENT) to A.G., and by the Agency for Management of University and Research Grants (AGAUR) of the Catalan Government grant 2017SGR01743. P.F. is supported by an AECC postdoctoral fellowship (POSTD211561FUEN), F.I. by an FPI fellowship (PRE2018-086310), C.M. by an FPU fellowship (FPU18/04400), and J.P. by Juan de la Cierva Fellowship (FJCI-2014-20422). V.M received funds from the Agency for Management of University and Research Grants (AGAUR) of the Catalan Government grant 2017SGR723 and the Spanish Association Against Cancer (AECC) Scientific Foundation. We thank CERCA Programme/Generalitat de Catalunya for institutional support.
Author contributions: This study was conceived and designed by A.G. A.G. performed most of the experiments together with P.F and J.P. C.M., F.I., T.R., and M.G. contributed to individual experiments. RNA-seq and TSS data were processed and analyzed by V.D.O. A.G. A.G., P.F., J.P., C.M., and F.I. analyzed the data. All authors provided intellectual support in the discussion of the results. A.G. guided the studies and wrote the manuscript. **Competing interests:** The authors declare that they have no competing interests. **Data and materials availability:** All data needed to evaluate the conclusions in the paper are present in the paper and/or the Supplementary Materials.

Submitted 4 February 2021
Accepted 6 October 2021
Published 26 November 2021
10.1126/sciadv.abg9275